Ital. J. Geosci., Vol. 139 (2020), pp. 76-97, 13 Figs. (https://doi.org/10.3301/IJG.2019.21)

Non-condensed shell beds in hiatal successions: instantaneous cementation associated with nutrient-rich bottom currents and high bivalve production

Adam Tomašových (1) , Ján Schlögl (2), Jozef Michalík (1) & Lenka Donovalová (2)

ABSTRACT

Pelagic carbonate deposits formed by the thin-shelled, epifaunal, originally bimineralic bivalve *Bositra buchi* were geographically widely distributed in the Tethyan basins during the Middle Jurassic. Here, to evaluate conditions that allowed the formation of peculiar, metre-scale, densely-packed shell beds primarily formed by *Bositra*, we assess size distributions and preservation of this bivalve in thin sections at ten sites in the Pieniny Klippen Belt and Peri-Klippen units (Western Carpathians), representing a bathymetric transect from pelagic-platform tops with shell beds up to slope environments where small filaments occur with spicules and radiolarians. Although *Bositra* shell beds are modulated by transport and winnowing, three types of evidence indicate that they primarily reflect high bivalve productivity. First, we find that size distributions of this species form a bathymetric gradient, from the dominance of remains smaller than 0.5 mm in low-energy slope environments, to 0.5-2 mm on muddy platform edges, up to lensoid shell beds with large valves (~2-15 mm) occurring on platform tops exposed to bottom currents. Although sediment winnowing from shell beds contributed to the rarity of small-sized specimens in platform-top environments, the bathymetric shift in the shape of size distributions is not purely driven by fragmentation and by size-selective transport of small specimens into slope environments because the average valve thickness declines with depth and thick fragments do not occur in slope environments. High abundances of suspension-feeding *Bositra* preferentially associated with indicators of bottom currents at oligophotic or aphotic depths indicate that plankton productivity was probably sourced by nutrient-rich internal waves that intersected platform tops, leading to low juvenile mortality in *Bositra* populations. In contrast, populations in deeper environments with the limited input of particulate organic matter failed to achieve maturity. Second, the inner, originally nacreous shell layer of *Bositra* is now represented by neomorphic calcite that is luminescent, enriched in Mn and depleted in Mg, indicating that this layer was not dissolved in the taphonomic active zone. Third, fibrous-acicular low-Mg calcite cements that characteristically coat *Bositra* in shell beds show blotchy luminescence and highly irregular Mg distribution, indicating that they were precipitated as high-Mg calcite cements. Fibrous-acicular cements in shell beds do not coat upward-facing sides of valves covered by a first phase of micrite whereas they fully coat elevated portions of the same valves. Therefore, they were precipitated at very high rates concurrently with micrite deposition in shelters. Nutrient-rich bottom currents thus simultaneously increased (1) *Bositra* survivorship by enhancing primary productivity and (2) cementation rate by renewal of saturation of pore waters in the taphonomic active zone at platform tops. In spite of the association of *Bositra* shell beds with major hiatal surfaces, (1) the rapid precipitation of fibrous-acicular cements, (2) the rarity of iron-stained *Bositra* valves in shell beds, and (3) the significantly smaller concentrations of iron in shell-rich muds than in shell-poor muds indicate that shell beds do not represent long-term hiatal or lag concentrations. They rather represent composite shell beds that record high population densities of these bivalves at ecological time scales. Spatial variation in intensity of bottom currents and in sea-floor topography generated by faulted blocks resulted (1) in hiatal surfaces with mineralized hardgrounds at high-energy current-swept sites and (2) in preservation of up to 1 m-thick lensoid shell beds at sites with less intense but persistent currents. *Bositra* shell beds thus ultimately have patchy horizontal and stratigraphic distribution.

Key words: *paleoecology, taphonomy, time averaging, shell beds, pelagic carbonate platforms.*

INTRODUCTION

The thin-shelled epifaunal bivalve *Bositra buchi* achieved a broad geographic range and represented one of the major rock-forming component of pelagic carbonate platforms during the Middle Jurassic. For example, it formed the so-called filament microfacies in the Middle Jurassic of the Eastern Atlantic (Jansa *et alii*, 1979; Steiger & Jansa, 1984; Steiner *et alii*, 1998), Eastern Alps (Krystyn, 1971; Böhm 1992; Ebli, 1997), Southern Alps (Sturani, 1971; Martire, 1992; Zempolich, 1993), Carpathians (Mišík, 1979; Aubrecht et alii, 2002; Schlögl *et alii*, 2005; Jach, 2007), Apennines (Santantonio, 1993, 1994; Conti & Monari, 1992), Sicily (Santantonio, 2002; Basilone *et alii*, 2010), Greece (Bernoulli & Renz, 1970; Harbury & Hall, 1988), and Betic Cordillera (Nieto *et alii*, 2012; Molina *et alii*, 2018). Other thin-shelled epifaunal pteriid bivalves, such as *Daonella* and *Halobia* in the Triassic (McRoberts, 2011), *Aulacomyella* in the Upper Jurassic (Kelly & Doyle, 1991), or other species during the Cretaceous (Negra *et alii*, 2011), also formed similar filament-like microfacies and shell beds in pelagic carbonate deposits. This recurrence indicates that some unique combination of oceanographic parameters, independent of species identity, repeatedly created favorable conditions for high abundance, broad geographic distribution, stratigraphic persistence, and rock-forming potential of these epibenthic bivalves with high dispersal abilities (Etter, 1996; Waller & Stanley, 2005). In contrast, however, this bivalve microfacies does not seem to have any clear ecological, taphonomic or sedimentological analogues in pelagic sediments of the Cenozoic or in present-day oceans. Therefore, oceanographic and depositional conditions that determined the dominance of this benthic life habit on pelagic carbonate platforms in the past remain enigmatic. Although oxygen depletion was a primary source of environmental disturbance (inducing high mortality of hypoxia-sensitive species

(1) Earth Science Institute, Slovak Academy of Sciences, Dúbravská cesta 9, 84005, Bratislava, Slovakia.
(2) Department of Geology and Paleontology, Comenius University, Mlynska dolina G, 84215, Bratislava, Slovakia.
Corresponding author e-mail: geoltoma@savba.sk

and allowing dominance of hypoxia-tolerant species such as *Bositra buchi*) in semi-enclosed epicontinental seas with the deposition of organic-rich shales during the Toarcian-Aalenian (Oschmann, 1994; Caswell & Coe, 2012; Monaco, 2016), the Bajocian (Erba *et alii*, 2019), or the Cenomanian-Turonian (Caron *et alii*, 2006), it is unclear what environmental factors contributed to the rock-forming abundance of filaments in organic-poor pelagic sediments formed in current-dominated and well-oxygenated pelagic environments.

On one hand, the filament microfacies with *Bositra buchi* is frequently represented by wackestones and packstones, typically in red nodular, pseudonodular or stromatactis-rich limestones deposited at aphotic depths (Martire, 1996; Aubrecht *et alii*, 2009), with minute and thin valve remains < 1 mm (short-filament microfacies of Kuhry, 1975; Kuhry *et alii*, 1976). On the other hand, larger shells (up to ~15 mm) can form unique, white-pink (sparitic), monospecific or paucispecific metre-scale shell beds (i.e., formed by densely-packed skeletal remains > 2 mm) that generated lensoid or mound-shaped banks, producing positive relief above seafloor, or dyke infills (long-filament microfacies, Sturani, 1967, 1971, Santantonio, 2002; Di Stefano *et alii*, 2002; Basilone, 2009; Molina *et alii*, 2018). Kuhry (1975) and Kuhry *et alii* (1976) postulated that the difference between short- and long-filament microfacies types reflects the effects of valve fragmentation and/or size-selective transport. In contrast, several authors suggested that shell beds with *Bositra* are unique ecological phenomena reflecting high primary productivity that sustained gregarious *Bositra* populations (Sturani 1967; Molina *et alii*, 2018) and/or that their superdominance on pelagic carbonate platforms can hint at stressful conditions or disturbances that excluded other benthic species (Navarro *et alii*, 2009).

The pelagic carbonate successions with the filament microfacies are, however, characterized by extreme condensation (Vera & Martin-Algarra, 1994; Clari *et alii*, 1995). This condensation was probably driven by a limited or non-existent input of sediments from phototrophic carbonate factories, unfavorable seawater chemistry, and/or strong currents that swept pelagic ridges and platforms (Bartolini & Cecca, 1999; Cecca *et alii*, 2005; Rais *et alii*, 2007). Therefore, it is unclear whether the abundance maxima of *Bositra* truly represent ecological blooms or outbreaks or whether the overall benthic production (and the flux of pelagic shells, including bivalve larval stages) rather reflects (1) a long-term attrition allowed by sediment starvation and/or (2) diagenetic residua that can be formed if less durable skeletal remains are dissolved early (Jach, 2007; Caron & Nelson, 2009; Cherns &Wright, 2009; Nohl *et alii*, 2018), especially when filaments occur in red stromatactis or nodular limestones that were deposited under conditions that led to the seafloor dissolution of aragonitic shells (Neuweiler & Bernoulli, 2005; Reolid *et alii*, 2010). High abundance of filaments (or abundance of other groups that were rock-forming during the Jurassic, such as planktonic foraminifers, radiolarians, or *Saccocoma*) thus can be exaggerated in condensed successions relative to their (not necessarily high) standing population size (Bellaiche & Thiriot-Quievreux, 1982). In such case, the lack of ecological analogues in the present-day oceans is less surprising.

However, fossil assemblages preserved in sediments bounded by hiatal surfaces are not necessarily significantly time-averaged and can be generated over temporal durations that are short relative to the total temporal duration encompassed by the corresponding hiatal surfaces. In such case, filament-rich beds can record ecological species pools rather than averaged pools of species from distinct stratigraphic zones (Kowalewski, 1996; Kowalewski & Bambach, 2008). In pelagic successions, this contrast is exemplified by the preservation of exceptionally preserved molluscan assemblages in sediment-filled fissures (dykes) that stratigraphically correspond to hiatal surfaces on the sea-floor (Schlögl *et alii*, 2009; Wendt, 2017) or by cemented shell beds rich in cephalopods that alternate with sediments containing less frequent but more altered and iron-stained cephalopod remains (Tomašových & Schlögl, 2008). To resolve the degree of time averaging of assemblages in *Bositra* shell beds, their sequence-stratigraphic context and association with hiatal surfaces, the residence time of shells in the taphonomic active zone, and the timing of cement formation need to be determined (Kidwell, 1988, 1989; Fürsich & Oschmann, 1993; Baeza-Carratalá *et alii*, 2014). Sedimentation rates are frequently intertwined with ecological and taphonomic factors that can increase or decrease shell production and preservation (Kidwell, 1986; Tomašových *et alii*, 2006; Brady, 2016, 2018). For example, on one hand, high sedimentation rates can suppress survivorship of epifaunal suspension-feeders but can enhance skeletal preservation rates by reducing the residence time of skeletal remains in the taphonomic active zone. On the other hand, low sedimentation rates coupled with rapid cement precipitation driven by bottom currents can enhance preservation rates. Therefore, analyses evaluating simultaneously variability in sedimentation, production and skeletal disintegration are needed to fully explain geographic and stratigraphic variation in the distribution of shell beds in carbonate settings and to assess their time averaging.

Here, we (1) assess stratigraphic and geographic distribution of *Bositra* shell beds and their relationship to hiatal surfaces in the Western Carpathians (Fig. 1), (2) disentangle the effects of taphonomic and ecological factors in generating a bathymetric gradient in shell size of *Bositra* on the basis of thin sections (i.e., microtaphofacies, MacLeod & Orr 1993; Tomašových & Schlögl 2008; Silvestri *et alii*, 2011; Jarochowska, 2012), and (3) evaluate the rate of precipitation and nature of cements that coat skeletal remains in *Bositra* shell beds. The Middle-Upper Jurassic successions in the Western Carpathians are characterized by very high condensation (Fig. 2), with two major hiatuses ocurring during the Late Bajocian and during the Callovian-Early Oxfordian (converging to a single hiatal surface in some sections), and thus provide opportunities for assessing time averaging of fossil assemblages in condensed successions.

SETTING

We quantified size distributions and preservation of *Bositra buchi* at ten Middle Jurassic sections in the Western Carpathians that belong to Czorsztyn Unit of the Pieniny Klippen Belt (Oravic Superunit) and to the peri-Klippen units (Drietoma and Manín units of the Fatric

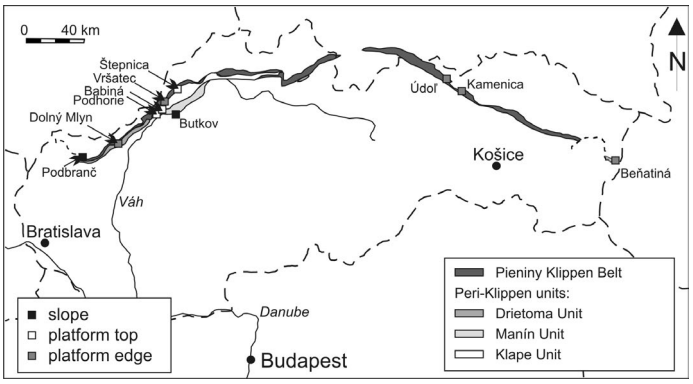

Fig. 1 - Geographic locations of ten sections (belonging to the Czorsztyn Unit) in the Pieniny Klippen Belt and two sections belonging to the Peri-klippen units (Butkov in the Manín Unit and Podbranč in the Drietoma Unit), coded according to their environmental affinity during the Middle Jurassic (platform top, platform edge, and slope).

Superunit) (Fig. 1). These tectonic units represent thrust sheets with a unique temporal, paleogeographic and paleoenvironmental evolution. The Pieniny Klippen Belt (PKB) represents a relict of a continental fragment in a Middle Penninic position (Plašienka, 2019). It is up to 600 km long and only a few km wide accretionary prism that was formed during the southward subduction of the European platform. The PKB was separated from the northern European shelf and segregated into the northern Czorsztyn Ridge swell and the southern Kysuca-Pieniny basin since the earliest Bajocian (Tyszka, 2001; Segit *et alii*, 2015). The western part of the Czorsztyn Ridge was located during the Middle Jurassic at ~20-25°N during the Bajocian and at ~25-35°N during the Callovian (Jeleńska *et alii*, 2011), whereas its eastern part was probably located at ~35-40°N during the Bajocian and at 25-30°N during the Callovian (Lewandowski *et alii*, 2005). The Kysuca-Pieniny Basin bordered on the southern margin with the Central Western Carpathians, including the peri-Klippen units (belonging to the Fatric Superunit, Plašienka, 2019) where the Middle Jurassic sediments are comparable to slope deposits rimming the southern slopes of the Czorsztyn Ridge (Wierzbowski *et alii*, 2004). During the Middle and Late Jurassic, the extensional regime led to the formation of fault-bounded swells and basins in the Pieniny Klippen Belt and in the Central Western Carpathians, with the mixture of condensed and redeposited sediments and the formation of escarpments, scarp breccias, and rapid horizontal changes in sediment thickness (Aubrecht & Szulc, 2006). The Czorsztyn Ridge is thus equivalent to depositional conditions that characterized the pelagic carbonate platforms from Apennines or Sicily (Santantonio, 1994; Basilone, 2009).

With the exception of a coral carbonate factory that was limited to the western part of the Czorsztyn Ridge during the early Bajocian (Ivanova *et alii*, 2019), crinoidal (sparite-dominated Smolegowa and micrite-dominated Krupianka formations) and crinoidal-spiculitic limestones (Flaki Formation) were deposited on the Czorsztyn Ridge during the Early and earliest Late Bajocian, followed by a hiatus in the Late Bajocian. The deposition of stromatactis-rich non-nodular limestones (Bohunice Formation; Aubrecht *et alii*, 2002, 2009) and red indistinctly-nodular (i.e., pseudonodular, sensu Martire, 1996) and nodular limestones of the Czorsztyn and Niedzica formations started in the latest Bajocian and continued up to the Kimmeridgian on the Czorsztyn Ridge. All these three formations are characterized by microfacies rich in filaments and/or globochaetes up to the Callovian. Benthic assemblages in these microfacies are almost exclusively formed by heterotrophic organisms (non-symbiontic foraminifers, brachiopods, crinoids, echinoids, and molluscs). The filament microfacies is abruptly replaced by the protoglobigerinid microfacies that is typical of the Oxfordian. In slope environments, the deposition of nodular limestones (Niedzica Formation) was replaced by radiolarian limestones and radiolarites (Czajakova Formation) with occurrences of calciturbiditic layers. Although the major phase of the deposition of radiolarian-rich sediments occurred in the Oxfordian, this replacement probably occurred already during the Callovian in the PKB and in the peri-Klippen units because *Bositra* filaments co-occur with radiolarians in basal parts of radiolarian limestones. The deepest basinal environments of the Kysuca-Pieniny Basin (not investigated here) are characterized by absence of the Middle Jurassic nodular limestones (i.e., radiolarites directly overlie Bajocian spiculitic or spiculitic-crinoidal limestones, e.g., Gedl, 2008).

METHODS

We assess maximum length, maximum thickness, and preservation of *Bositra* remains in thin sections along a bathymetric transect in the Pieniny Klippen Belt (Czorsztyn Unit) and in two peri-Klippen units (Drietoma and Manín units, Figs. 1-2). We assign these sections to three environments differing in (1) water depth, (2) their exposure to bottom currents on the basis of differences in the proportion of micrite and (3) presence of redeposits and radiolarian sediments. First, sparite-rich crinoidal limestones (Smolegowa Formation) and the overlying stromatactis-rich limestones with abundant crinoids and brachiopods (non-nodular Bohunice and Štepnica formations and successions with horizontal transitions between non-nodular and nodular formations) preserved at Babiná, and Podhorie, and Štepnica (Mišík *et alii*, 1994; Aubrecht *et alii*, 2002; Schlögl *et alii*, 2009; Aubrecht & Jamrichová, 2009) are assigned to platform-top environments. Second, reddish micrite-rich crinoidal limestones (Krupianka Formation) and the overlying pseudonodular and nodular limestones of the Czorsztyn Formation (filament and globochaete wackestones and packstones) preserved at Vršatec, Údoľ, Kamenica, Beňatina, and Dolný Mlyn (Schlögl *et alii*, 2005) are assigned to platform-edge environments. Third, allodapic crinoidal limestones and spiculitic limestones (Flaki Formation), nodular limestones of the Niedzica Formation, and radiolarian mudstones and wackestones (Czajakova Formation) preserved at Butkov (Manín Unit, Borza *et alii*, 1987) and Podbranč (Drietoma Unit, Michalík *et alii*, 1999) are assigned to slope environments. In addition, we focus on the stratigraphic context of two lensoid shell beds with *Bositra* (attaining 1 m in thickness) formed by white sparitic rudstones at the Štepnica section (Fig. 3). These two shell beds bound the so-called Štepnica Formation (formed by massive crinoidal-brachiopod packstones and grainstones) on the bottom and on the top.

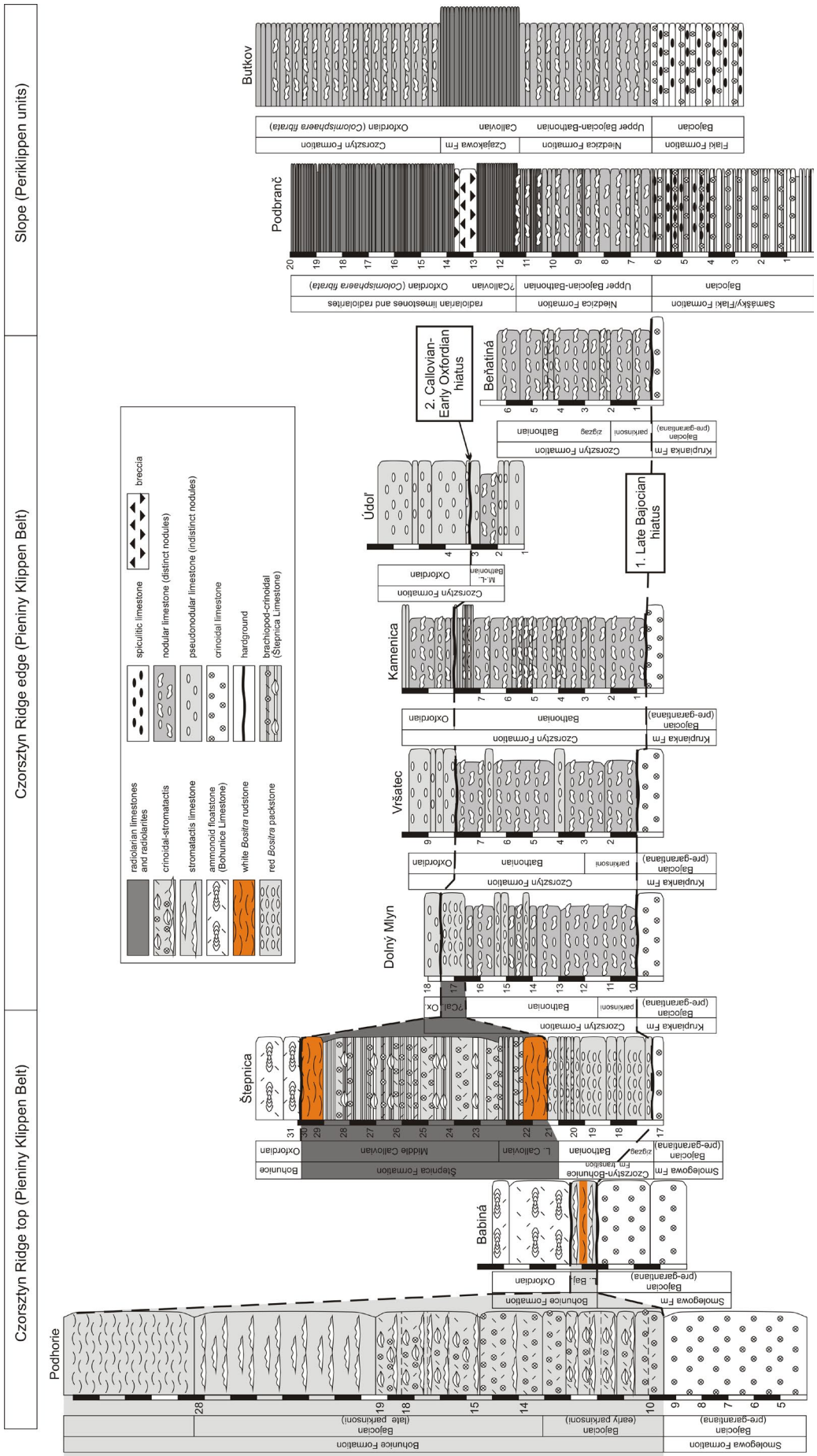

Fig. 2 - The geographic transect in facies composition from platform tops with stromatactis-rich and coquinal brachiopod-crinoidal limestones (Podhorie, Babiná, Štepnica) to platform edges with nodular limestones (Dolný Mlyn, Vršatec, Kamenica, Údoľ, and Beňatiná) up to slope environments (Podbranč and Butkov). This transect shows two major hiatuses that formed during the Late Bajocian and during the Callovian-Early Oxfordian. Platform-top sections tend to be thicker and preserve to some degree the deposits that are missing on platform edges, including thick Upper Bajocian-Lower Bathonian sediments at Podhorie that correspond to a single stromatactis layer at Babiná, and the Lower-Middle Callovian deposits at Štepnica that are time-equivalent to a subset of the Callovian-Early Oxfordian hiatus in all other sections. Two marked shell beds with *Bositra* bound the Callovian deposits at Štepnica. Gray-colored beds possess reddish micritic matrix and white-colored beds are sparitic. The Butkov section is simplified on the basis of the schematic description in Borza et al. (1987); other sections are based on bed-by-bed descriptions.

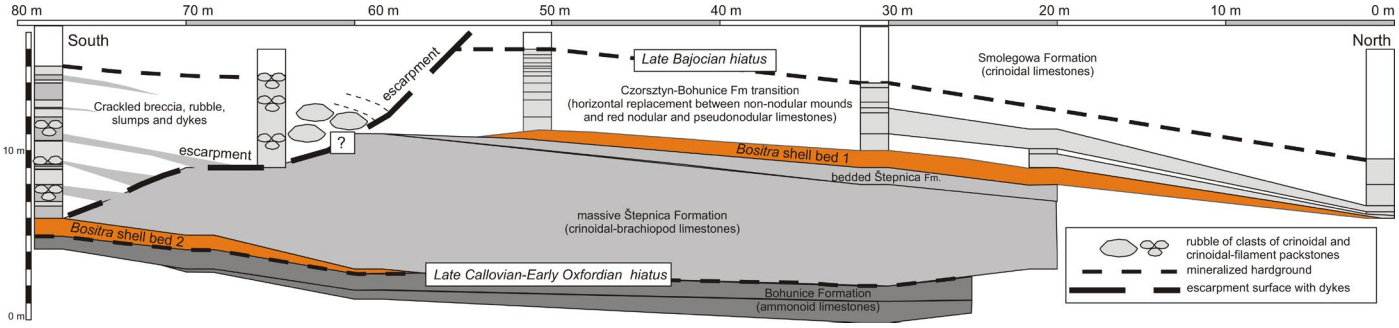

Fig. 3 - A transect view of Štepnica section (stratigraphically overturned) that represents a single section in the Pieniny Klippen Belt where the Callovian non-dyke sediments (Štepnica Formation) are directly dated by ammonites. The Štepnica Formation is represented by a sedimentary wedge overlying (1) the paleoescarpment formed by crackled and rubble breccias on the top of the southern fault block (penetrated by dykes filled by sediments from the Štepnica Formation) and (2) the nodular and pseudonodular limestones in the northern part (hangingwall of the northern fault block). Two *Bositra* shell beds form two lenses that bound the Štepnica Formation on the base and on the top.

Measuring and interpreting size of valves in thin sections is coupled with two difficulties. First, lengths of *Bositra* remains in thin sections inevitably underestimate their true length. Although size distributions are approximations biased towards small sizes, large differences in their shape along bathymetric gradients can be informative about the underlying gradients in size. Second, size distributions can vary as a function of bathymetric gradients in intensity of fragmentation and sorting rather than due to ecological gradients in population size structure. To control for the effects of fragmentation and size-selective transport on the shape of size distributions, we also measure the thickness of valves. Although specimens of *Bositra* are extremely thin (Jefferies & Milton, 1965), discrimination between small-sized individuals and small fragments derived from larger valves is allowed by a subtle ontogenetic increase in valve thickness: minute convex specimens of *Bositra* that are < 0.5 mm long have valves that are <0.01 mm thick whereas the thickness of individuals > 1 mm exceeds 0.015-0.02 mm. Although these thickness estimates are affected by uncertainty generated by differences in the orientation of valves, high abundance of thin and short fragments contrasts with the rarity of thick short fragments in slope environments, indicating that short-filament microfacies is not purely generated by fragmentation of larger specimens and/or by size sorting.

In total, the length and thickness of 12,007 specimens of *Bositra* in 125 thin sections was measured. Each specimen was scored for presence of isopachous cements at 10x magnification under the light-microscope. The lengths of specimens refer to the their maximum length in thin sections. The proportion of cementation per thin section refers to the number of specimens with cement rims relative to the total number of specimens.We analyse size distributions of *Bositra* remains in thin sections on the basis of log-transformed length. We use non-metric multidimensional scaling and Frechet distance, with length bins spanning 0.25 logarithmic units (in mm). We use permutational multivariate analysis of variance (PERMANOVA, Anderson, 2001) to assess differences in size distributions among three environments (platform top, platform edge, and slope). The minimum sample size in analyses is 30 specimens per thin section. The measurements of length and thickness are available in Supplementary Table 1.

Bositra buchi precipitated bimineralic valves, with the outer prismatic calcitic layer and the inner aragonitic nacreous layer (Jefferies & Minton, 1965; Conti & Monari 1992). To assess the preservation of these layers and their relationship to isopachous cements, we analysed the chemical composition of *Bositra* valves, of fibrous-acicular and blocky cements that fill voids among *Bositra* valves in shell beds, and of micritic sediment in two, shell-rich and shell-poor samples (a biosparitic shell bed at the Štepnica-22 with the long-filament microfacies, and a filament-rich biomicritic wackestone at Beňatiná-12 with the short-filament microfacies) with wave-dispersion X-ray microanalysis and backscattered electrons (BSE), using a JXA-8530F electron microprobe (Supplementary Table 2). Operating conditions were 10 µm spot resolution, 15 kV accelerating voltage and 15-20 nA sample current. The relative standard deviation is less than ± 5 %. The natural standards used in analyses were diopside for Ca (Kα, PETL), celestite for Sr (Kα, TAP), albite for Na (Kα, TAP), diopside for Mg (Kα, TAP), hematite for Fe (Kα, LIFH), and rhodonite for Mn (Kα, LIFH). Concentrations of Ca, Mg, Sr, Mn and Fe were measured along three transects crossing *Bositra* valves and isopachous cements coating these valves in the shell bed (Štepnica-22). Cathodoluminescence (CL) and scanning electron microscope (SEM) analyses were also performed on these two thin-sections. The CL photomicrographs of *Bositra* shells were performed using hot CL-microscope HC2-LM (Simon-Neuser) at the Masaryk University, Brno, Czech Republic. Observations were carried out at 15 keV accelerating voltage, beam current of 0.2 mA and the overall magnifications from 4x to 10x.

RESULTS

Association of Bositra shell beds with hiatuses

Crinoidal packstones and grainstones with dispersed valves of *Bositra* were deposited during the Bajocian at all sites on the Czorsztyn Ridge (prior to the *Garantiana garantiana* Zone, Fig. 2). The crinoidal limestones rich in sparite are overlain by non-nodular, stromatactis-rich wackestones and floatstones with crinoids, brachiopods, and

Bositra (Bohunice and Štepnica formations) in platform-top environments in the western part of the Pieniny Klippen Belt (Aubrecht *et alii*, 2002, 2009). Non-nodular mounds with stromatactis structures are horizontally replaced by beds with indistinct and distinct nodules over several meters at Štepnica (i.e., the Bohunice Formation horizontally passes into the Czorsztyn Formation at this location). *Bositra* shell beds in these platform-top environments are typically represented by white sparitic rudstones. The crinoidal limestones rich in micrite are overlain by red pseudonodular and nodular limestones (with distinct and indistinct nodules initially generated by bioturbation) in platform-edge (Czorsztyn Formation) and slope environments (Niedzica Formation, Fig. 2). *Bositra* shell beds in these platform-edge environments are typically represented by red micritic packstones with concordantly oriented valves and indistinct nodularity. Spiculitic-crinoidal wackestones and packstones with *Bositra* were deposited during the same time in slope environments at Podbranč and Butkov (Borza *et alii*, 1987) and in slope environments of the Pieniny Klippen Belt (Wierzbowski *et alii*, 2004). *Bositra* shell beds do not occur in slope environments.

The boundary between crinoidal limestones (Krupianka Formation) and nodular limestones (Czorsztyn Formation) in platform-edge sections is invariably formed by a Fe-rich hardground with *Frutexites* and ammonite shells with complex taphonomic history characterized by repeated burial, lithification, and exhumation (correlation line 1 in Fig. 2). The oldest ammonites in nodular limestones of the Czorsztyn Formation point either to the *Parkinsonia parkinsoni* Zone or to the *Zigzagiceras zigzag* Zone (at Štepnica), indicating that this hiatus spans at least one or two ammonite zones (Wierzbowski *et alii*, 1999, 2004; Schlögl *et alii*, 2005). We refer to this hiatal surface as the Late Bajocian hiatus.

Nodular and pseudonodular limestones of the Czorsztyn Formation are characteristically bounded by a second major hiatal surface associated with a mineralized hardground, marked by an abrupt replacement of the filament wackestones and packstones (Bathonian or Callovian) by the protoglobigerinid wackestones and packstones (Oxfordian, correlation line 2 in Fig. 2). With the exception of the Štepnica section, sediments of the Callovian age are either missing or extremely condensed on the Czorsztyn Ridge (and only preserved in dykes in other sections in the Pieniny Klippen Belt, Schlögl *et alii*, 2009). This hiatus can also incorporate the Late Bathonian, but for simplicity, we refer to it as the Callovian-Early Oxfordian hiatus. In contrast to the Czorsztyn Ridge, the Callovian sediments in slope environments (at Podbranč and Butkov) are represented by radiolarian-filament mudstones and wackestones, occasionally with breccias. These two (Late Bajocian and Callovian-Early Oxfordian) hardgrounds are separated just by a single, 1 m-thick stromatactis bed with brachiopods at Babiná, with an about 10 cm-thick *Bositra* rudstone (shell bed) in the middle part. Although ammonites in this bed were not found, this bed contains a similar brachiopod assemblage as at Podhorie where a massive stromatactis-rich succession dated by ammonites corresponds to the uppermost Bajocian and Lower Bathonian (Aubrecht *et alii*, 2009).

On the basis of ammonite occurrences, the Callovian-Lower Oxfordian hiatal surface passess into a ~9-10 m-thick sedimentary wedge (Štepnica Formation, bedded limestones in the lowermost part and massive limestones in the upper part) at Štepnica (gray-shaded sector in Fig. 2), where this wedge is bounded on the bottom and the top by two ~ 1 m-thick *Bositra* shell beds (white rudstones, Fig. 3). This wedge is formed by non-nodular brachiopod-crinoidal deposits that accumulated on a stepped margin formed by two blocks separated by a fault. These brachiopod-crinoidal deposits were thus deposited in a depression underlain partly by a paleoescarpment (in the southern part) and on the top of the hangingwall block (in the northern part, Fig. 3). Both *Bositra* shell beds possess lensoid, mound-like shape, with a relatively flat base and a convex, low-relief upper surface, attain 100-110 cm in thickness at maximum, and are developed over several tens of meters (Fig. 3). The lower *Bositra* shell bed (Štepnica 22 below) immediately overlies pseudonodular limestones formed by filament wackestones and packstones (Czorsztyn Formation). This bed completely pinches out both in the southern and northern direction. In the southern part, it passes into a steep paleoescarpment on the top of a crackled and rubble breccia (Fig. 3). Ammonites in the bedded part of the Štepnica Formation overlying the first shell bed indicate the *Bullatimorphites bullatus* Zone, i.e., the lower shell bed is of Late Bathonian or Early Callovian age. The upper *Bositra* shell bed (Štepnica 30 below) is developed in the uppermost part of this wedge and is bounded on the top by a mineralized (Upper Callovian-Lower Oxfordian) hardground, overlain by ammonite floatstones of the Bohunice Formation (Middle Oxfordian). Ammonites in the massive part of the Štepnica Formation indicate the Lower and Middle Callovian (*Macrocephalites gracilis* and *Erymnoceras coronatum* Zones, Schlögl *et alii*, 2009). To conclude, *Bositra* shell beds are bounded by hiatal surfaces (at Babiná and Štepnica) or horizontally pinch out to hiatal surfaces that represent time-equivalent (especially Callovian) subsets of sedimentary successions at other sites of the Czorsztyn Ridge.

Bositra size distributions and preservation

Size distributions of *Bositra* form a marked gradient that correlates with bathymetric configuration of ten sections (Fig. 4-6). First, left-skewed size distributions with high abundance of specimens > 2 mm, comparable to the long-filament microfacies of Kuhry (1975), occur in floatstones with dispersed *Bositra* and especially in white rudstone shell beds that were formed in platform-top environments (Fig. 4A-B). At Podhorie and Štepnica, large valves of *Bositra* are also dispersed in stromatactis or crinoidal-brachiopod floatstones and packstones and thus do not necessarily always form densely-packed shell beds. In addition to left-skewed distributions that are typical of shell beds, size distributions that represent a bimodal mixture of larger specimens and abundant silt-sized but relatively thick (~0.02 mm) comminuted debris also occur in some portions of shell beds (Fig. 4C, Fig. 5). Second, red filament wackestones and packstones of the Czorsztyn Formation deposited in platform-edge environments are characterized by symmetric, normal-shaped size distributions, with abundant small specimens but also with a significant portion of specimens between 1-2 mm (Fig. 4D). Third, occurrences associated with spiculitic, globochaete and radiolarian mudstones, wackestones,

and packstones (slope environments) are characterized by dominance of specimens < 0.5 mm and by absence of specimens > 1 mm, forming right-skewed size distributions (4F). The last two types of distributions are comparable to the short-filament microfacies of KUHRY (1975).

The cm-scale stratigraphic variability in size of *Bositra* within the two shell beds at Štepnica shows that they are composite in nature, reflecting multiple rather than a single depositional event. Although they do not show any signs of grading or cross-stratification, they consist of cm-scale alternation of lenses or layers that differ in the shape of size distributions (from left-skewed to bimodal distributions), in abundance of micrite, in the degree of fragmentation, and in valve orientation that ranges from nested valves oriented in concave-up position up to chaotically-oriented valves. However, convex-up oriented valves are rare. In some case, the comminuted debris from larger valves even generates right-skewed distributions (Štepnica at 29.75 m in Fig. 5).

The size of *Bositra* specimens in thin sections consistently decreases from platform-top environments towards slope environments: the mean size (per thin section) is on average equal to 0.25 mm in slope

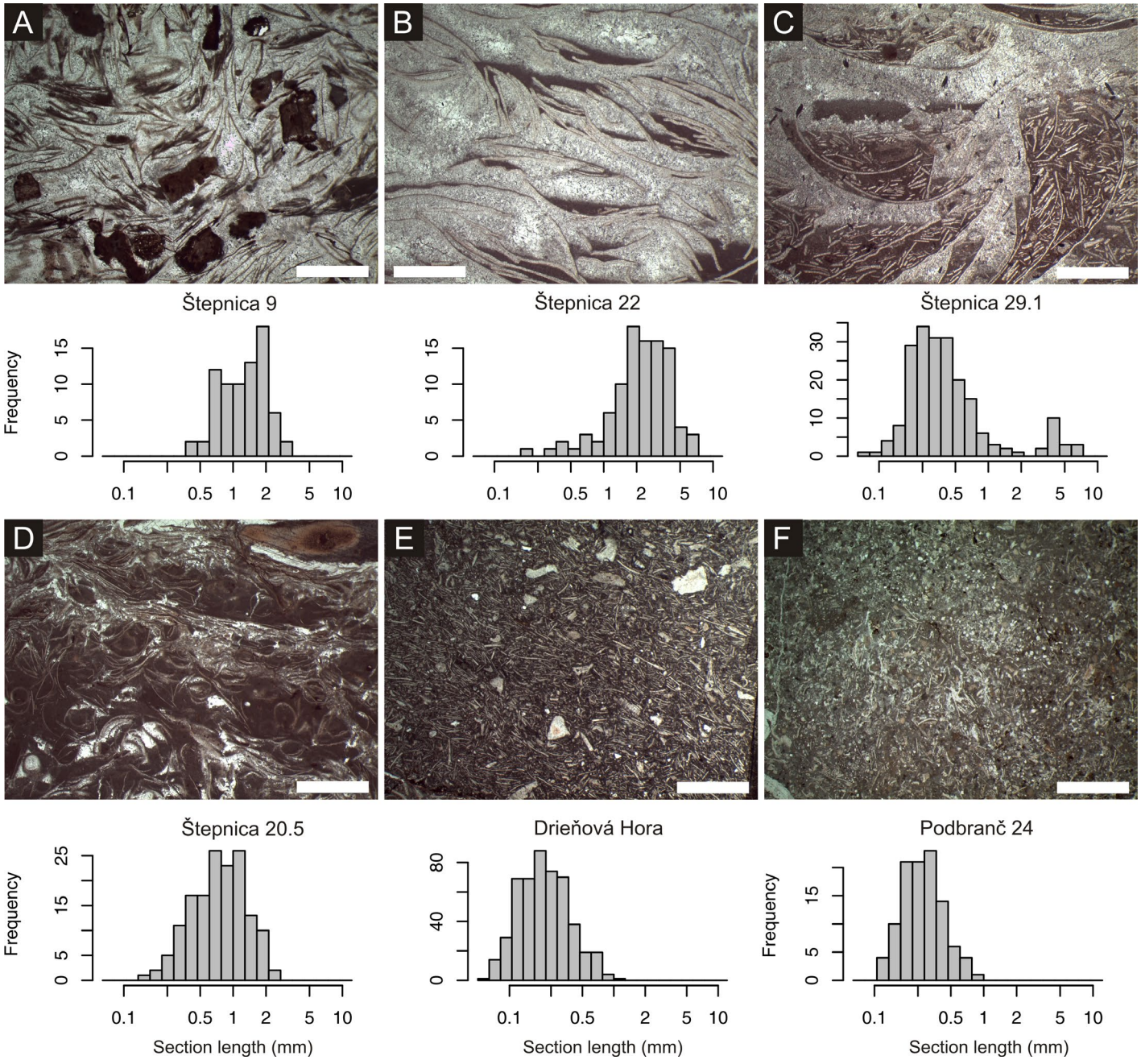

Fig. 4 - Microfacies types that capture a general bathymetric gradient in the shape of size distributions of *Bositra*, from left-skewed distributions dominated by specimens that are larger than 2 mm (rudstone shell beds, A-B), bimodal distributions with a mixture of larger shells and comminuted debris (derived from larger shells) that are also typical of shell beds (C), symmetric distributions with specimens attaining 0.5-2 mm, typical of wackestones and packstones of filament wackestone and packstones (red nodular or pseudonodular limestones) (D), and more right-skewed distributions with specimens smaller than 0.5 mm typical of spiculitic, globochaete and radiolarian wackestones (E-F). The scale bar: 2 mm.

environments (i.e., right-skewed distributions) and exceeds 0.5 mm or more in platform-top environments (i.e., left-skewed distributions). The 95th percentile size is on average 2 mm on platform tops, 1 mm on platform edges, and 0.5 mm on slopes. In general, this bathymetric gradient in size of *Bositra* persisted from the Late Bajocian up to Callovian, although the decline is steeper in the Upper Bajocian and in the Callovian than in the Bathonian (Fig. 6A). The largest shells occur in crinoidal-brachiopod floatstones (with stromatactis structures) and rudstones dominated by *Bositra* (Fig. 6B). Spiculitic and radiolarian wackestones are characterized by the smallest specimens. Crinoidal packstones, filament packstones, and globochaete wackestones and packstones show intermediate size distributions (Fig. 6B). The bathymetric gradient in size structure is also detected by multivariate

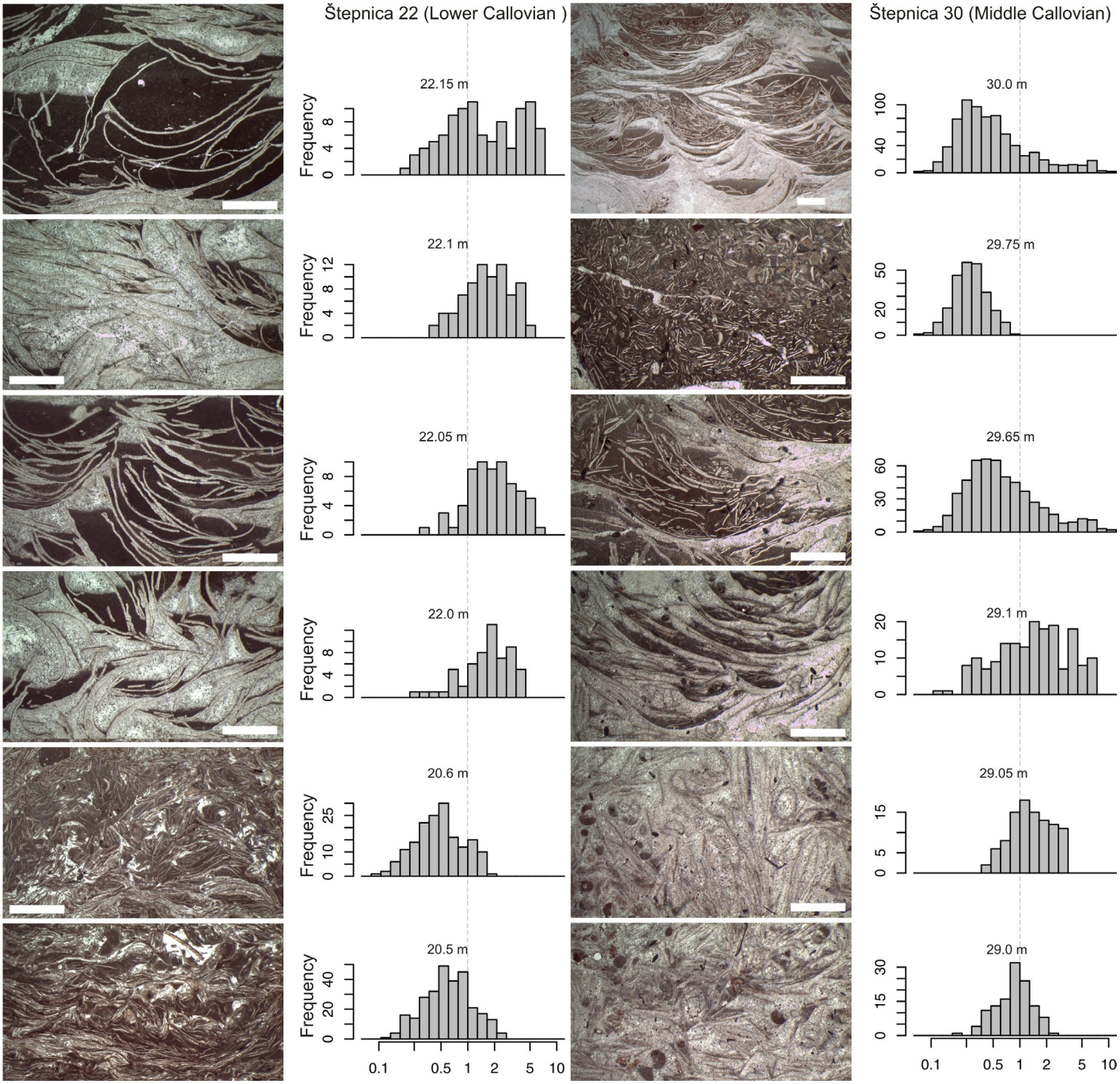

Fig. 5 - Internal variability in size of *Bositra* within two (rudstone) shell beds at Štepnica. The shell bed at 22 m (Lower Callovian) is underlain by well-sorted filament packstones (20.5 m) with symmetric size distributions. Shell-bed rudstones show relatively homogeneous distributions dominated by larger individuals. Lenses with densely-packed nested valves in concave-up orientations and partial micritic infills alternate with lenses where micrite is rare and most voids are filled by fibrous and blocky cements. Distributions become bimodal owing to abundance of comminuted debris in the upper parts. The shell bed at 10 m (Middle Callovian) is characterized by higher heterogeneity, with altered bioclasts (crinoids, brachiopods, *Bositra*) on the basis, and cm-scale alternation of layers with left-skewed and bimodal distributions. The scale bar: 2 mm.

analyses (PERMANOVA, F [top vs. edge] = 28.9, $p < 0.001$; F [top vs. slope]= 36.2, $p < 0.001$; F [edge vs. slope]= 10.3, $p < 0.001$), with the proportion of cohorts < 0.5 mm ranging from less than 10% in platform-top shell beds up to more than 90% in slope sediments (Fig. 6C).

The proportion of valves coated by cement rims increases towards shallower environments (Fig. 6D). The percentage of cemented valves is > 50% in shell beds, on average about 20% in crinoidal, crinoid-brachiopodal and filament wackestones and packstones, and less than 5% in globochaete, spiculitic and radiolarian wackestones and packstones. The median, minimum and maximum thickness of *Bositra* valves is consistently smaller in slope environments than on platform tops and edges (Fig. 7A). The thin specimens are rare or missing on platform tops and edges whereas the thicker specimens do not occur in slope environments. This lack of thick fragments in deep environments cannot be explained by taphonomic effects (Fig. 7B).

Bositra valves in wackestones and packstones frequently show iron-stained bioerosion (Fig. 8A and B), which is also a characteristic attribute of preservation of crinoids, cephalopods and brachiopods in micritic sediments of the pelagic carbonate platforms at our sites and in other regions (e.g., Reolid *et alii*, 2010; Preat *et alii*, 2011). In contrast, the frequency of bioerosion and staining is smaller or completely absent in rudstones (Fig. 8C-D). Closely-spaced couplets of equally-long and thick valves can be frequently observed in thin sections from Štepnica

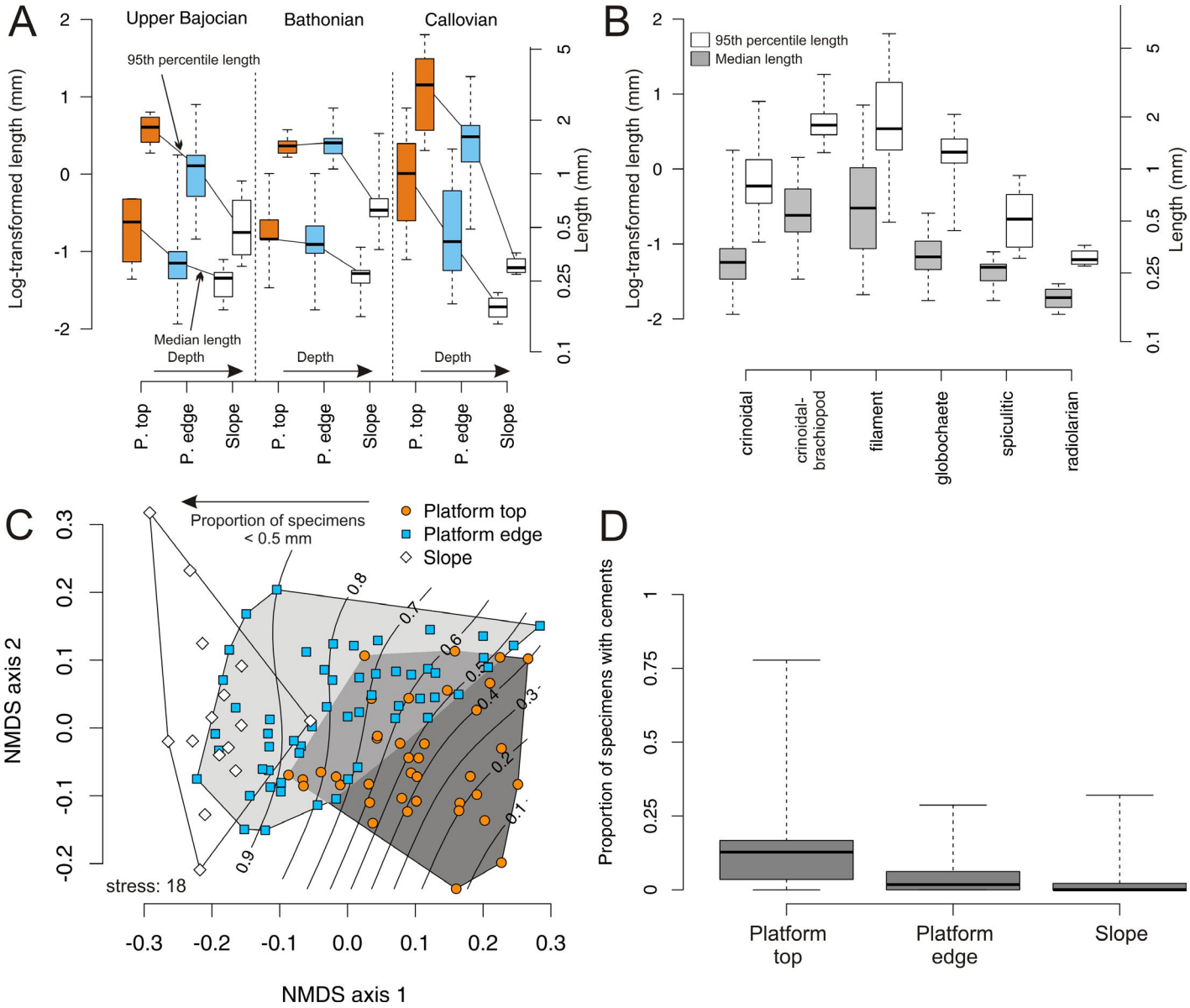

Fig. 6 - A. The bathymetric decline in the median log-transformed length (gray boxplots) and in the 95th percentile logged length (white boxplots) characterizes all three stratigraphic intervals. The boxplots are based on medians and 95th percentiles estimated for individual thin sections. B. Differences in size structure among six microfacies types. C. Non-metric multidimensional scaling showing bathymetric dependence of size distributions of *Bositra buchi*, with significant segregation among three environments (PERMANOVA, F=26.2, p < 0.001). The contours depict the proportion of specimens smaller than 0.5 mm that gradually increases with increasing depth towards slope environments. D. Boxplots showing proportions of specimens with fibrous cements in three environments, documenting a declining trend in cementation with depth.

and Dolný Mlyn, indicating that such remains represent valves from a single individual. Although *Bositra buchi* did not possess hinge teeth, this type of preservation indicates that some individuals were rapidly buried or diagenetically stabilized soon after their death.

Preservation of Bositra and cements

Focusing on specimen sections longer than 1 mm, *Bositra* valves are either dull, with small bright patches (Fig. 9A), or the outer layer is nonluminescent whereas the inner layer tends to be bright (white and black arrows in CL views in Fig. 9C-D, with corresponding light-microscope views in Fig. 9E-F). The smallest and very thin valves (< 0.5 mm) tend to show bright luminescence. In contrast, brachiopod valves are non-luminescent (Fig. 9B) and fragments of gastropods and planktonic foraminifers are luminescent. The internal heterogeneity in the degree of luminescence between the inner and outer portions in *Bositra* is consistent with the distribution of elemental concentrations (Figs. 9G-J, 10A-B), with higher concentrations of Mn and Sr in the inner layer. Scanning electrone microscope images show that the outer layer shows relicts of prisms and the inner layer is recrystallized both in filament wackestones and in shell beds (Fig. 10C-F). Therefore, the internal, originally-aragonite layer is neomorphic rather than dissolved.

Bositra specimens in shell beds are characteristically coated by cements that can be subdivided into two phases according to light-microscope, CL, and elemental analyses. They are both non-ferroan (Fe < 100 ppm) but strongly differ in the concentrations of Mg and Mn, including (1) Mn-poor fibrous-acicular cement (forming either very thin rims or thicker crusts) with highly variable Mg concentrations and (2) Mn-rich blocky cement with low Mg concentrations. Thin isopachous cements (0.025-0.04 mm in thickness) formed by fibrous crystals (length/width ratio varies between 2-6, Fig. 8C-F) tend to grow on one or both sides of *Bositra* valves. We note that isopachous rims formed by fibrous cement are also a characteristic attribute of *Bositra* preservation in the Middle Jurassic shell beds in other Tethyan regions (Kalin & Bernoulli, 1984, Clari & Martire, 1996, Aubrecht, 1997, Martire *et alii*, 2006). These rims of fibrous isopachous cements coat the valves on both sides only if valves are not covered by a first phase of sediment infill formed by light-gray micrite (Fig. 8C-D). Valve portions covered by light gray micrite are cement-free on their upward-facing side but elevated portions of the same valve are coated by thin isopachous rims. These thin rims can be either covered by the second phase of darker micritic sediment (Fig. 8) or they continuously pass into longer, inclusion-rich fibrous-acicular crystals (length/width ratio is between 6-15), with radial extinction pattern, and crystals up to 0.5 mm long (Figs. 10E-F and 11A-B). These fibrous crystals are characterized by patchy meshwork of light-gray and dark-gray spots (10-50 µm in size) under the BSE (Fig. 11) and by blotchy luminescence (Fig. 12A-B), giving this cement phase a characteristic spotted or patchy appearance (Fig. 11). Microprobe maps (Fig. 12E-G) and transects (Fig. 13)

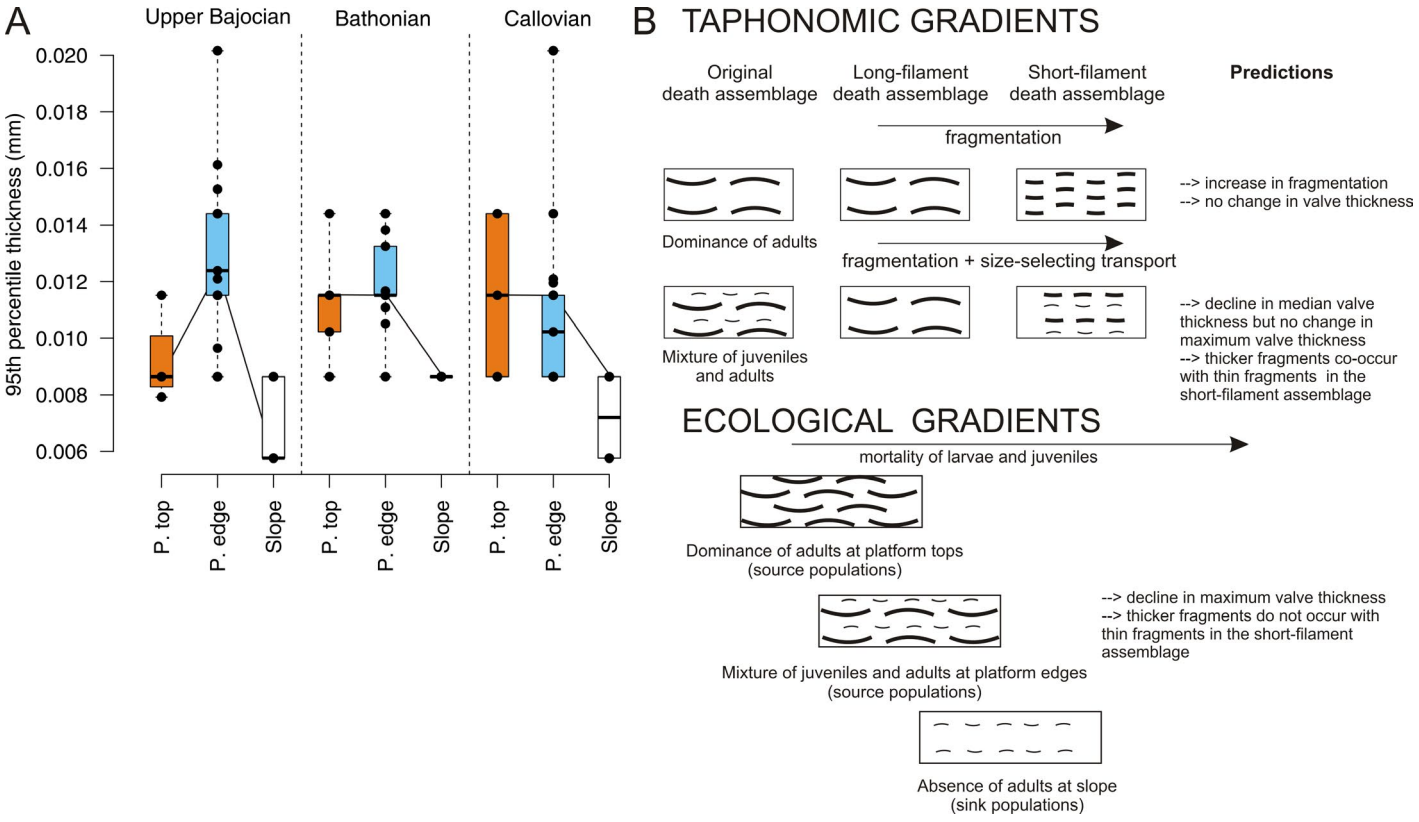

Fig. 7 - A. The bathymetric decline in the 95th percentile valve thickness (per thin section) characterizes all three stratigraphic intervals. B. Conceptual predictions for taphonomic scenarios generating gradients in size structure of *Bositra* specimens contracts with predictions when the gradients in size structure are generated by ecological gradients in size-specific mortality.

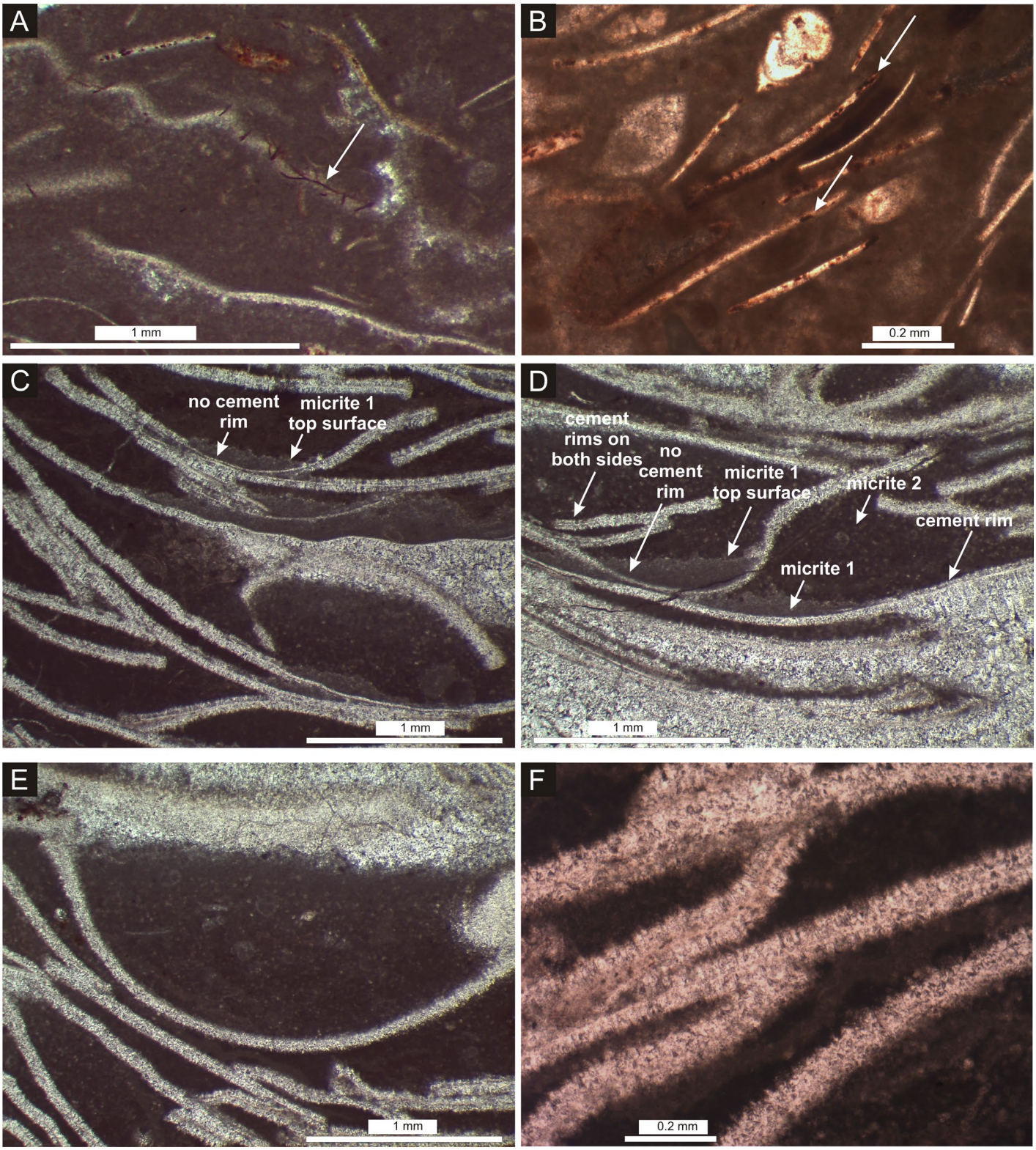

Fig. 8 - Bositra with bioerosion and *Bositra* with thin isopachous rims of fibrous crystals under the light microscope. A – dispersed valves affected by Fe-stained borings (pointing with arrows). Štepnica 20.5 m. B – stained borings within fragments of *Bositra* (pointing with arrows) co-occurring with stained and bored crinoids on the basis of the upper shell bed at Štepnica (29.1 m). C-E – the relationship between micrite and thin isopachous rims on *Bositra* valves: the lowermost parts of former pores among valves are covered by a first generation of micritic sediment (light-gray micrite 1). The upper, elevated valve portions not buried by this first-generation micrite are coated by thin fibrous cements on their upward-facing side. These isopachous rims of fibrous cement are covered by a second generation of micrite (dark gray micrite 2). F – *Bositra* valves coated by isopachous rims on both sides.

show that this patchiness is generated by variability in the concentration of Mg, fluctuating between 1,000 and 5,000 ppm across few micrometers (Fig. 13). A blocky cement with bright luminescence and high Mn content and locally also higher Sr content (and low Mg content) represents the final phase of filling of cavities between *Bositra* valves (Figs. 11-13). The concentrations of Fe in reddish, shell-poor micrites (wackestones) of nodular limestones without any cements (1,500-2,500 ppm, Fig. 8M) are much higher than concentrations of Fe in a gray micrite that partly fills cavities among *Bositra* valves in the shell beds (less than 150 ppm). Microdolomite

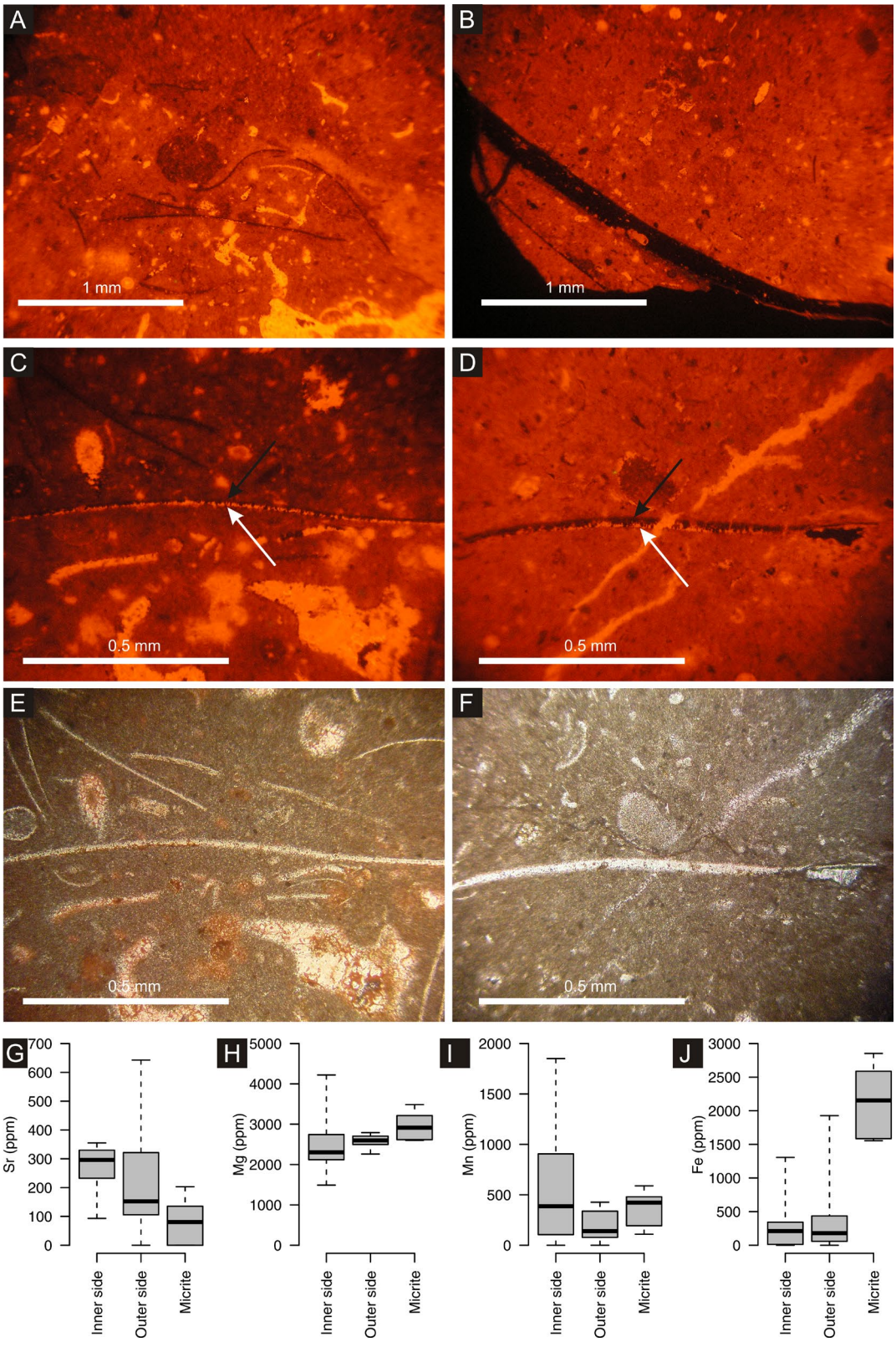

Fig. 9 - Preservation of Bositra in CL and light-microscope views (filament wackestone at Beňatiná). A-B – Nonluminescent valves of *Bositra* (~ 1 mm in length) dispersed in a micritic matrix (A) and a brachiopod valve affected by bioerosion (B). C-D - *Bositra* valves showing non-luminescent outer side (black arrow) and luminescent inner side (white arrow). The smallest valves shorter than 0.3 mm in A are luminescent. E-F – the same sections in the light-microscope view. G-J – microprobe results showing that the internal (luminescent) sides of *Bositra* valves are enriched in Sr and Mn relative to outer sides. The concentrations of Fe are markedly higher in micrite than in valves.

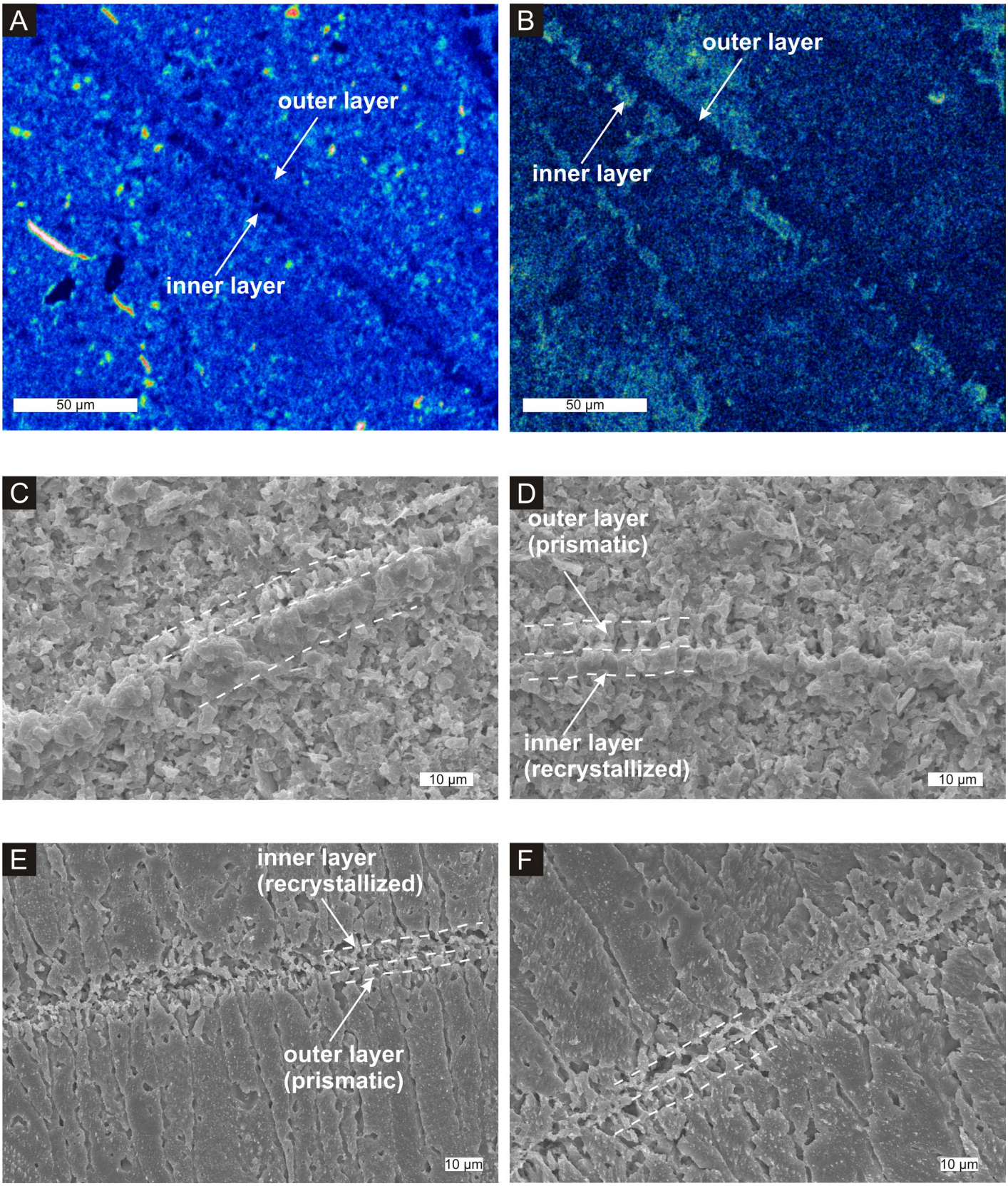

Fig. 10 - Electron microprobe (EPMA, A-B) maps and scanning electrone microscope images (SEM, C-F) showing the relicts of two-layer shell structure of very thin filaments (~20 µm) of *Bositra* in the filament wackestone (red nodular limestones, Beňatiná 12). A. The inner layer is depleted in Mg. B. The inner layer is enriched in Mn. C-D. Cross-sections of *Bositra* in the shell-poor filament wackestone (Beňatiná 12) show that the outer layer shows relicts of prisms and the inner layer is recrystallized . E-F. Cross-sections of *Bositra* with the inner (recrystallized) and outer (prismatic) layers in the shell bed (Štepnica 22).

inclusions are not present.

DISCUSSION

Bathymetric gradients in mortality

The bathymetric gradient in size did not shift in time and remained a rather persistent feature of *Bositra* populations because stratigraphic changes in size of valves (from Upper Bajocian up to Callovian) within the three environments remain relatively constant. Kuhry *et alii* (1976) suggested that fragmentation and transport are major controls of variation in size distributions of *B. buchi*. Although winnowing in platform-top environments probably contributed to the rarity of small specimens, the size-selective transport can be expected to mix thicker fragments of originally larger specimens with thinner fragments of smaller specimens in slope environments. Therefore, the absence of larger specimens in slope environments cannot be explained by sorting of fragmentation (Fig. 7B). In addition, bimodal distributions with high abundance of short but thick fragments in some sectors of shell beds (in platform-top environments) rather reduce the steepness of the bathymetric decline in size. Therefore, we suggest that the size gradient is at least partly driven by bathymetric shifts in size-selective mortality that were related to changes in the exposure of bivalve habitats to bottom currents.

Relationship between primary productivity and bottom currents

Benthic assemblages almost exclusively formed by heterotrophic guilds in stromatactis, nodular and pseudonodular limestones with the filament microfacies indicate that they inhabited oligophotic or aphotic depths on the Czorsztyn Ridge where bottom currents can be sourced by nutrient-rich internal waves that propagate along pycnoclines and break against the slope of topographic highs (Pomar *et alii*, 2019). The populations with larger, mature individuals of *Bositra* that preferentially inhabited the current-exposed platform tops of the Czorsztyn Ridge thus probably benefited from an increase in current flow (e.g., van Erkom Schurink & Griffiths, 1993) and locally-enhanced plankton productivity (see also Molina *et alii*, 2018) relative to populations inhabiting deeper and low-energy habitats. The bathymetric shifts in size structure were thus probably driven by a decrease in larval and juvenile mortality towards habitats with nutrient-rich bottom currents that fueled high plankton productivity. These conditions can be comparable to current-exposed hard-bottom habitats colonized by suspension-feeding bivalves benefiting from nutrient-rich currents at permanent pycnoclines in present-day environments. For example, the epibyssate bivalve *Acesta* forms dense populations in aphotic seamount environments where strong currents at density boundaries enhance nutrient concentrations and primary productivity (Lopez Correa *et alii*, 2005; Johnson *et alii*, 2013). The cementing oyster *Neopycnodonte* forms dense biostromes on steep walls at the nutrient-rich interface between the Eastern North Atlantic Water and the Mediterranean Outflow Water (Van Rooij *et alii*, 2010). Buildups with abundant suspension-feeders at outer shelves in the geological past were also explained by the coupling between currents and high plankton productivity at depths intersected by nutrient-rich internal waves at pycnoclines (Pomar *et alii*, 2012). High primary productivity is the main factor that contributes to the carbonate-forming potential of molluscs in Holocene environments (Vermeij 1990; Taylor *et alii*, 1997; Reijmer *et alii*, 2012; Klicpera *et alii*, 2015; Michel *et alii*, 2018), and we suggest that it can explain the volumetric dominance of *Bositra* in the Middle Jurassic shell beds as well.

Bathymetric decline in primary productivity

The co-occurrence of filaments with radiolarians in the slope environments at Podbranč and Butkov is most likely coeval with the development of *Bositra* shell beds at Štepnica during the Callovian. Even when the acme of radiolarian deposition occurred during the Oxfordian in the PKB (when platform-top sediments are represented by protoglobigerind microfacies), the deposition of sediments rich in radiolarians started already during the late Bajocian in the deepest parts of the Tethyan basins (Baumgartner *et alii*, 1995). Primary productivity near the Czorsztyn Ridge was thus probably positively influenced by high nutrient concentrations that fueled primary productivity and thus also high abundance of radiolarians in open surface waters of the western Tethys already since the late Bajocian (Baumgartner, 2013). Jach (2007) suggested that the replacement of microfacies rich in *Bositra* by radiolarians can signify a shift towards high primary productivity during the late Middle Jurassic in the Central Western Carpathians, with the dominance of filaments during the Bajocian-Early Bathonian and with the dominance of radiolarians during the Late Bathonian and Callovian (Jach *et alii*, 2014). However, the dominance of *Bositra* on platform tops during the Callovian, concurrently with high abundance of radiolarians that formed radiolarian microfacies in slope and basinal environments, indicates that filament and radiolarian microfacies are primarily differentiated in terms of their proximity to pelagic swells and by the differences in the efficiency of the export of particulate organic matter to the seafloor in the deeper environments. Regardless of whether the surface mixing layer in the Tethys Ocean was characterized by high primary productivity and/or plankton productivity was further enhanced by internal waves near pelagic carbonate platforms, the export of particulate organic matter to deeper benthic environments (where it can be used by suspension-feeding bivalves) was probably limited during the Middle Jurassic, contributing to the mortality of juveniles or unsuccessful larval settlement of *Bositra* in deeper, platform-edge environments, and especially in slope environments. Therefore, we suggest that the size distributions in slope environments primarily reflect sink populations that died prior to their maturity, sourced from the propagule pressure generated by healthy populations in shallower environments not limited by food supply.

Taphonomic pathways and early-diagenetic stabilization of Bositra in shell beds

Early-diagenetic dissolution in the taphonomic active zone can eliminate aragonitic bioclasts from

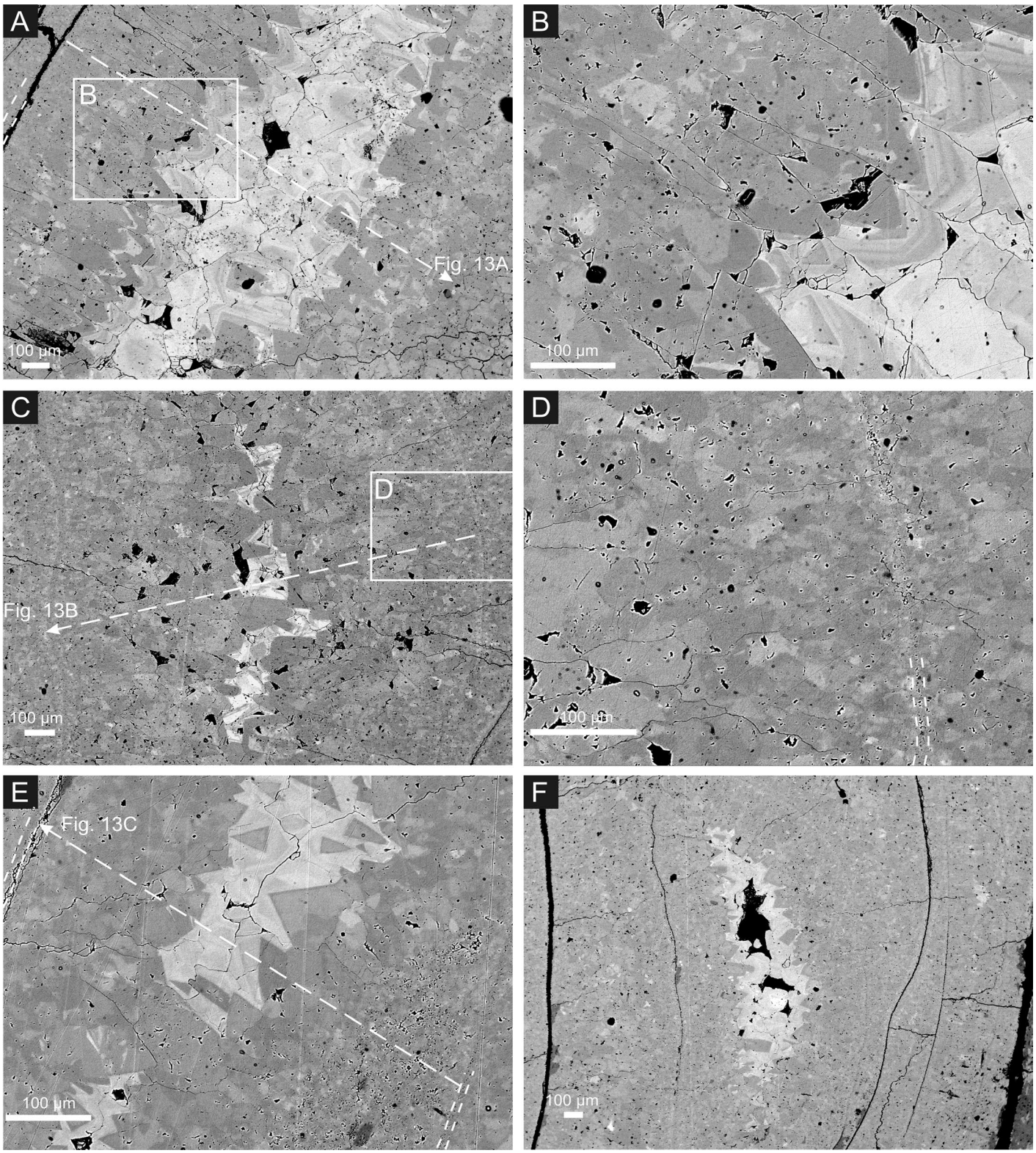

Fig. 11 - The backscattered electron (BSE) images of three transects through cements enclosed between *Bositra* valves showing that the fibrous-acicular cement phase is characterized by patchiness formed by irregular meshwork of dark-gray (rich in Mg) and light-gray (depleted in Mg) patches. On the transition to the center, fibers show small-scale zonality, and the center of cavities is filled by light gray cements. The location of three transects plotted in Figure 13 is shown by white arrows. *Bositra* valves are demarcated by white dashed lines.

fossil assemblages in pelagic carbonate deposits (Rivas *et alii*, 1997). Such pathway may have biased assemblage composition towards the dominance of *Bositra* relative to aragonite producers (Jach, 2007), especially in nodular and pseudonodular limestones that are characterized by the moldic preservation of ammonoids (Coimbra & Oloriz, 2012; Reolid et alii, 2015). However, larger *Bositra* valves are still formed by two layers that differ in microstructure

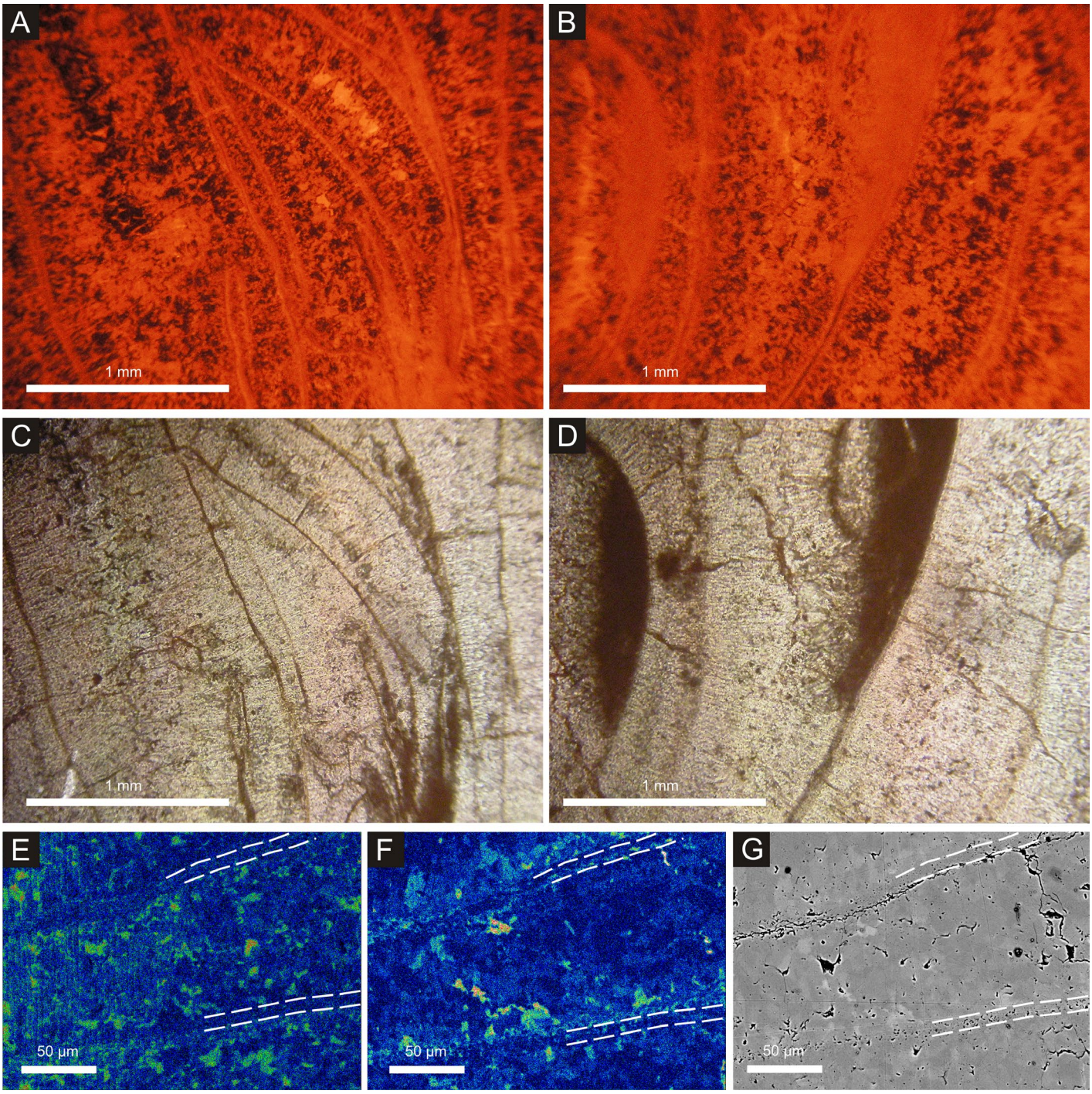

Fig. 12 - Preservation of *Bositra* and cements in the shell bed (Štepnica 22) in CL (A-B) and light-microscope views without polarised light (C-D). Two phases of cementation can be distinguished, including (1) fibrous-acicular cements with blotchy luminescence, and (2) luminescent blocky cement filling the innermost voids. The fibrous-acicular cement shows a radial extinction pattern. Microprobe maps show highly-variable concentrations of Mg (E) and less variable concentrations of Mn (F) in fibrous cements between two valves of *Bositra* (lighter colors correspond to higher concentrations). The BSE image (G) shows the location of two valves demarcated by white dashed lines.

and elemental concentrations. The originally-aragonitic portions were thus not dissolved (and were later replaced by neomorphic low-Mg calcite) and both layers (rather than just a calcitic layer) passed through the taphonomic active zone, both in shell beds and in microfacies with higher proportion of micrite (e.g., red nodular and pseudonodular limestones). However, ammonoids co-occurring with filaments in the Czorsztyn and Niedzica formations are typically represented by reworked molds (Schlögl *et alii*, 2005), clearly suggesting that some aragonite dissolution occurred in the taphonomic active zone prior to the final burial on the Czorsztyn Ridge. To explain this paradox, we hypothesize that those *Bositra* valves that were subjected to the selective dissolution of aragonitic layer in the taphonomic active zone rapidly disintegrated into minute fragments, especially on muddy

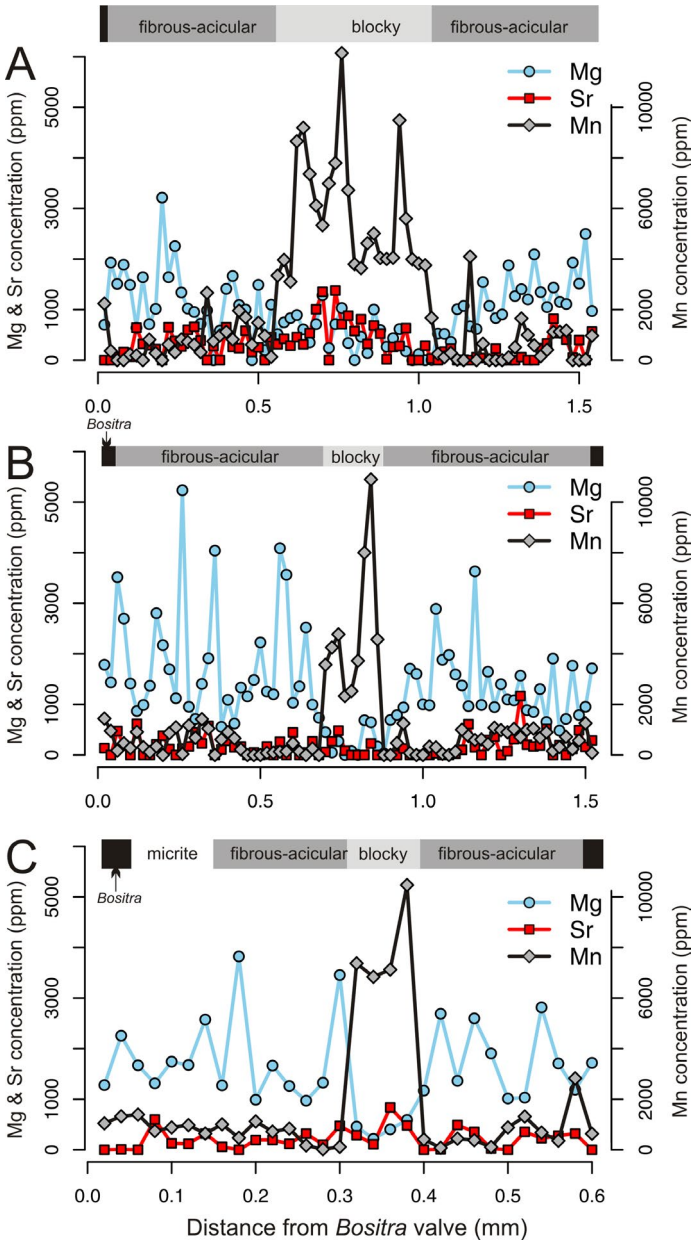

Fig. 13 - Three transects with concentrations of Mg, Sr, and Mn (measured with electron microprobe), passing through cement-filled cavities bounded by *Bositra* valves on both sides (*Bositra* shell bed, Štepnica 22), show that the fibrous-acicular cements possess highly variable concentrations of Mg. The blocky cement is consistently enriched in Mn and depleted in Mg, indicating that the shift from fibrous to blocky cements reflects a decline in redox potential due to enhanced solution of Mn^{2+} in anaerobic pore waters and its incorporation into calcite.

bottoms with intense bioturbation. Such fragments were either fully degraded or are so small so that they cannot be identified as remains of *Bositra* valves anymore.

In micrite-rich sediments, disintegration of larger specimens of *Bositra* in the taphonomic active zone seems to be driven by fragmentation, staining, and bioerosion. In contrast, *Bositra* valves in shell beds are rarely stained or bored. Instead, they were characteristically coated by thin isopachous rims of fibrous cements. The juxtaposition between the micrite covering the lowermost portions of valves and the precipitation of fibrous cement on elevated valve portions not covered by micrite indicates that the these rims must have been precipitated very quickly, concurrently with the deposition of micrite that was sheltered from winnowing. The rate of precipitation of calcite cement can be very high in present-day bathyal environments, with a growth of several µm-thick crusts occurring at yearly scales (Grammer *et alii*, 1999). The shift from fibrous cements with patchy luminescence to Mn-rich luminescent cements indicates that initial rims were formed under aerobic pore-water conditions, and redox conditions shifted towards reducing conditions in the final phases of void filling (Hendry, 1993; Reinhold & Kaufmann, 2010), further indicating that fibrous cements precipitated rapidly under the active influence of bottom currents.

Micrometer-scale patches depleted in Mg within individual crystals and the blotchy luminescence patterns indicate that the fibrous-acicular cements were originally formed by high-Mg calcite cements (Budd, 1992; Mazzullo *et alii*, 1990; Bruckschen *et alii*, 1992). Isopachous fibrous cements or similar cements with blotchy luminescence, inferred to initially represent high-Mg calcite cements, were also forming during the Middle Jurassic on the Burgundy Platform, in the Paris Basin or in the High Atlas Basin (Durlet & Loreau, 1996; Brigaud *et alii*, 2009; Pierre *et alii*, 2010; Andrieu *et alii*, 2017). Isopachous fibrous cements that are rich in inclusions, show blotchy luminescence and coat skeletal remains are also characteristic of high-Mg calcite that precipitated during the Cenozoic (James & Bone, 1991; Major & Wilber, 1991; Nelson & James, 2000; Knoerich & Mutti, 2003; Caron *et alii*, 2005). The loss of Mg and the neomorphic replacement of the inner layer of *Bositra* by calcite represent the last steps in the diagenetic sequence that occurred during the burial.

Time averaging of shell beds

The absence or rarity of iron-stained *Bositra* valves in shell beds, which is a typical attribute of bioclasts in shell-poor microfacies of the Czorsztyn, Štepnica and Bohunice formations, suggests that the *Bositra* shell beds were formed over decades or few centuries rather than over several millennia. Iron staining is also a characteristic and pervasive attribute of preservation of crinoids, cephalopods and brachiopods on hiatal surfaces associated with significant biostratigraphic condensation in pelagic carbonate sediments in other regions (e.g., Reolid *et alii*, 2010; Preat *et alii*, 2011). A direct dating of cephalopod shells from present-day bathyal environments shows that multi-centennial residence time of skeletal particles on the sea-floor can be required to generate stronger alteration and staining (Tomašových et al., 2017) and iron-stained relicts of Holocene and Pleistocene mollusks are older than several millenia on cool-water carbonate shelves (Rivers *et alii*, 2008). However, with the exception of the lowermost parts of the upper shell bed at Štepnica where stained *Bositra* valves are present, the staining does not characterize *Bositra* remains in shell beds. We thus suggest that (1) the relationship between the earliest cement rims and micrite in shell beds, (2) the low proportions of bored valves in shell beds, and (3) the low concentrations of iron in shell beds (in contrast to shell-poor but iron-rich sediments without cements) demonstrate that *Bositra* shell beds accrued rapidly and that processes leading to shell disintegration and alteration in the taphonomic active zone were rather inactive in shell beds. This scenario

contrasts with a highly-reactive taphonomic active zone in shell-poor and bioturbated (nodular) deposits in pelagic carbonate environments, characteristically allowing the alteration and formation of iron-stained skeletal remains (Tomašových & Schlögl, 2008; Preat *et alii*, 2011; Coimbra & Olóriz, 2012; Coimbra *et alii*, 2015). The timespan over which *Bositra* shell-bed assemblages were generated thus does not correspond to the timespan encompassed by hiatuses (i.e., the timespan of at least one ammonite zone, > 500,000 years up to few Myr).

Bottom currents triggering condensed surfaces and non-condensed shell beds

Hiatal surfaces with hardgrounds that were formed on the northwestern Tethys shelf and on the pelagic ridges during the Callovian are typically explained by strong and persistent currents that swept sediment to deeper basins (Rais *et alii*, 2007). Clari & Martire (1996) documented that cementation on the pelagic carbonate platforms, with the deposition of nodular limestones and *Bositra*-rich sediments, was effectively related to flushing of the sediment-pore systems in the taphonomic active zone by currents (supplying a near-sea floor pore systems with carbonate ions) rather than to alkalinity buildup driven by anaerobic organic-matter degradation and sulphate reduction in iron-rich sediments (Dickson *et alii*., 2008; van der Kooij *et alii*, 2010). Anaerobic decomposition can lead to high pH and promote carbonate preservation and early cementation, but precipitation of cements on *Bositra* valves clearly occurred under aerobic conditions. Such conditions can favor the precipitation of high-Mg calcite cements, which frequently form in association with condensed surfaces when sediment bypassing and erosion is triggered by bottom currents, precipitating from marine waters undersaturated with respect to aragonite (Saller, 1986; Knoerich & Mutti, 2003).

The lensoid, mound-like shape of shell beds indicates that they can represent low-relief skeletal banks modulated by mud-winnowing bottom currents (e.g., Santantonio *et alii*, 1996) that can be triggered in pelagic environments by internal waves that propagate along pycnoclines (Pomar *et alii*, 2012). Nested, concave-up orientations of *Bositra* valves in shell beds indicate that they settled out of the suspension, probably from turbulent flows that can be driven by breaking of internal waves (Pomar *et alii*, 2019) against topographic complexities that characterize pelagic swells (e.g., Lueck & Mudge, 1997; Dorschel *et alii*, 2014). However, *Bositra* shells were not redeposited or reworked after the fibrous rims formed because the present-day stratigraphic orientation of cements and mud shelters remains consistent with their initial growth orientation. Transport distances were probably not high because (1) our macroscopic examinations of *Bositra* valves on bedding surfaces of shell beds indicate that the majority of valves above 1-2 mm are complete and (2) the left-skewed distributions with large individuals are limited in their bathymetric distribution to platform tops (i.e., larger individuals were not transported to deeper settings). The shell beds that are 1 m-thick ultimately record multiple events of shell deposition (not far from their life habitat), small-scale bioturbation that locally generated bimodal size distributions with a mixture of thick fragments and larger specimens and small patches with differing degree of packing (but not sufficiently extensive to disturb concave-up oriented valves in other portions of shell beds), and rapid cementation.

The cement formation was probably enhanced by bottom currents on the Czorsztyn Ridge because the proportion of valves with cement rims declines towards low-energy slope habitats and the cement zonality indicates that their initial precipitation occurred under aerobic conditions. We thus suggest that this action of bottom currents led not only to the formation of hiatuses with significant stratigraphic gaps (> 500,000 years up to few Myr), but was also responsible for the formation of shell beds at locations affected by currents not too strong to remove skeletal particles (or to rework or erode densely-packed framework of *Bositra* valves after the isopachous rims were formed) but sufficiently persistent to allow mud winnowing and rapid cementation.

The probability of cement formation was probably contingent on initial size distribution of *Bositra* valves (prior to cementation) because accumulations of smaller valves may not have allowed a stable framework with sufficiently large and interconnected pores that allow current flushing associated with renewal of alkalinity and removal of products from organic decay (James *et alii*, 1976). Only specimens with larger valves can allow the persistence of shelly framework. Therefore, ecological factors allowing higher survivorship (and thus production of larger valves) probably feedback into the probability of shell-bed preservation. Bimodal size distributons with a large number of comminuted fragments indicate that some valves disintegrated into many fragments due to bioturbation occurring prior to cement formation, leading to dense or loose packing of fragments without cements.

Geographic and stratigraphic patchiness in the distribution of shell beds

Sturani (1967) observed that shell beds with *Bositra* occur in extremely localized patches and that they correspond to distinct ammonite zones rather than containing ammonites from multiple zones. Such patchy distribution can be expected under spatially-complex topography induced by the development of faulted blocks, leading to differences in base level owing to spatial differences in the intensity of bottom currents. At platform tops, such currents probably not only enhanced primary productivity but also determined whether individual locations were exposed to strong currents or breakdown of internal waves that led to sediment bypassing and erosion or whether they were sheltered, with currents intense enough to remove small particles and promote cementation but not strong enough to produce erosion, and thus allowed for the preservation of shell beds. We suggest that this complexity explains the spatially-variable formation and preservation of shell beds that pinch out and pass into current-swept hiatal surfaces, without any sediment preserved. This geographic and stratigraphic patchiness is in accord with our observations: two major shell beds with *Bositra* have lensoid, mound-like appearance and occur at two distinct stratigraphic intervals, at times when the coeval sediments are represented by hiatal surface in other sections (Figs. 2 and 3). However, this patchiness translates to long-term persistence at broader, basinal scales, i.e., source populations generating propagule pressure were

always present on pelagic platforms as evidenced by persistence of abundant small-sized specimens in the filament microfacies in deeper environments.

CONCLUSIONS

Bositra shell beds are not diagenetic relicts and record high abundance of epifaunal filter-feeding bivalves at ecological time scales uniquely associated with enrichment in food supply and with instantaneous cementation at tops of pelagic carbonate platforms. Hydrodynamic conditions that enhanced primary productivity (at platform tops as opposed to bathyal benthic habitats) also actively removed fine material and promoted almost instantaneous precipitation of fibrous high Mg-calcite. The filament microfacies with smaller *Bositra* valves in slope environments reflect high larval and juvenile mortality. Although shell beds are overlain by hardgrounds or are horizontally replaced by escarpment surfaces or hardgrounds that span one or more ammonoid zones, they are not stratigraphically condensed themselves. Their geographic and stratigraphic patchiness is probably driven by variability in the intensity of bottom currents induced by irregular sea-floor topography. The signs of rapid cementation and the rarity of iron staining as well as low concentrations of iron in shell-bed micrites (as opposed to high iron concentrations in shell-poor micrites) indicate that time averaging of *Bositra* shell beds is rather decadal or centennial. *Bositra* shell beds thus represent examples of non-condensed, within-habitat time-averaged facies that occur in open ocean-margin successions with strong bottom currents and significant hiatuses.

ELECTRONIC SUPPLEMENTARY MATERIAL

This article contains electronic supplementary material which is available to authorised users.

Acknowledgments

We thank to Marco Brandano, Jose Miguel Molina, and Idoia Rosales for critical reviews and Sergii Kurylo and Tomáš Mikuš for help with microprobe measurements. This work was supported by the Slovak Research and Development Agency (APVV-17-0555, APVV-17-0170) and the Slovak Scientific Grant Agency (VEGA01/0169/19).

REFERENCES

Anderson M.J. (2001) - *A new method for non-parametric multivariate analysis of variance*. Austral Ecol., **26**, 32-46.

Andrieu S., Brigaud B., Barbarand J. & Lasseur E. (2017) - *Linking early diagenesis and sedimentary facies to sequence stratigraphy on a prograding oolitic wedge: the Bathonian of western France (Aquitaine Basin)*. Mar. Petrol. Geol., **81**, 169-195.

Aubrecht R. (1997) - *Indications of the middle Jurassic emergence in the Czorsztyn unit (Pieniny Klippen belt, Western Carpathians)*. Geol. Carpath., **48**, 71-84.

Aubrecht R., Szulc J., Michalík J., Schlögl J. & Wagreich M. (2002) - *Middle Jurassic stromatactis mud-mound in the Pieniny Klippen Belt (Western Carpahtians)*. Facies, **47**, 113-126.

Aubrecht R. & Szulc J. (2006) - *Deciphering of the complex depositional and diagenetic history of a scarp limestone breccia (Middle Jurassic Krasin Breccia, Pieniny Klippen Belt, Western Carpathians)*. Sediment. Geol., **186**, 265-281.

Aubrecht R., Schlögl J., Krobicki M., Wierzbowski H., Matyja B.A. & Wierzbowski A. (2009) - *Middle Jurassic stromatactis mud-mounds in the Pieniny Klippen Belt (Carpathians)—a possible clue to the origin of stromatactis*. Sediment. Geol., **213**, 97-112.

Aubrecht R. & Ožvoldová L. (1994) - *Middle Jurassic–Lower Cretaceous development of the Pruské Unit in the western part of the Pieniny Klippen Belt*. Geol. Carpath., **45**, 211-223.

Aubrecht R. & Jamrichová M. (2009) - *Štepnická skala Klippe–unique type of the Czorsztyn Succession (Pieniny Klippen Belt, Western Carpathians)*. Acta Geol. Slov., **1**, 141-158.

Baeza-Carratalá J.F., Giannetti A., Tent-Manclús J.E. & Garcia-Joral F. (2014) - *Evaluating taphonomic bias in a storm-disturbed carbonate platform: effects of compositional and environmental factors in lower Jurassic brachiopod accumulations (eastern Subbetic basin, Spain)*. Palaios, **29**, 55-73.

Bąk M., Chodacka S., Bąk K. & Okoński S. (2018) - *New data on the age and stratigraphic relationships of the Czajakowa Radiolarite Formation in the Pieniny Klippen Belt (Carpathians) based on the radiolarian biostratigraphy in the stratotype section*. Acta Geol. Pol., **68**, 1-20.

Bartolini A. & Cecca F. (1999) - *20 My hiatus in the Jurassic of Umbria-Marche Apennines (Italy): carbonate crisis due to eutrophication*. C. R. Acad. Sci. IIA, **329**, 587-595.

Basilone L. (2009) - *Mesozoic tectono-sedimentary evolution of Rocca Busambra in western Sicily*. Facies, **55**, 115-135.

Basilone L., Morticelli M.G. & Lena G. (2010) - *Mesozoic tectonics and volcanism of Tethyan rifted continental margins in western Sicily*. Sediment. Geol., **226**, 54-70.

Baumgartner P.O., Martire L., Gorican S., O'Dogherty L., Erba E. & Pillevuit A. (1995) - *New Middle and Upper Jurassic radiolarian assemblages co-occurring with ammonites and nannofossils from the Southern Alps (Northern Italy)*. Mémoires de Géologie, **23**, 737-750.

Baumgartner P.O. (2013) - *Mesozoic radiolarites–accumulation as a function of sea surface fertility on Tethyan margins and in ocean basins*. Sedimentology, **60**, 292-318.

Bellaiche G. & Thiriot-Quievreux C. (1982) - *The origin and significance of a thick deposit of pteropod shells in the Rhône deep sea fan*. Palaeogeogr. Palaeoclimatol. Palaeoecol., **39**, 129-137.

Bernoulli D. & Renz O. (1970) - *Jurassic carbonate facies and new ammonite faunas from western Greece*. Eclogae Geol. Helv., **63**, 573-607.

Böhm F. (1992) - *Mikrofazies und Ablagerungsmilieu des Lias und Dogger der nordöstlichen Kalkalpen*. Erlanger Geol. Abh., **121**, 57-217.

Borza K., Michalík J. & Vašíček Z. (1987) *Lithological, biofacial and geochemical characterization of the Lower Cretaceous pelagic carbonate sequence of Mt. Butkov (Manín Unit, West Carpathians)*. Geol. Carpath., **38**, 323-348.

Brady M. (2016) - *Middle to upper Devonian skeletal concentrations from carbonate-dominated settings of North America: Investigating the effects of bioclast input and burial rates across multiple temporal and spatial scales*. Palaios, **31**, 302-318.

Brady M. (2018) - *Testing patterns of association between brachiopod bioclast deposits and stratigraphic discontinuities: A case study in middle–upper Devonian carbonate-dominated settings of North America*. J. Geol., **126**, 141-164.

Brigaud B., Durlet C., Deconinck J.F., Vincent B., Thierry J. & Trouiller A. (2009) - *The origin and timing of multiphase cementation in carbonates: Impact of regional scale geodynamic events on the Middle Jurassic Limestones diagenesis (Paris Basin, France)*. Sediment. Geol., **222**, 161-180.

Bruckschen P., Neuser R.D. & Richter, D.K. (1992) - *Cement stratigraphy in Triassic and Jurassic limestones of the Weserbergland (northwestern Germany)*. Sediment. Geol., **81**, 195-214.

Budd D.A. (1992) - *Dissolution of high-Mg calcite fossils and the formation of biomolds during mineralogical stabilization*. Carbonate. Evaporite., **7**, 74-81.

Caron M., Dall'Agnolo S., Accarie H., Barrera E., Kauffman E.G., Amédro F. & Robaszynski F. (2006) High-resolution stratigraphy of the Cenomanian–Turonian boundary interval at Pueblo (USA) and wadi Bahloul (Tunisia): stable isotope and bio-events correlation. Geobios, **39**, 171-200.

Caron V., Nelson C. S. & Kamp P. J. (2005) - *Sequence stratigraphic context of syndepositional diagenesis in cool-water shelf carbonates: Pliocene limestones, New Zealand.* J. Sediment. Res., **75**, 231-250.

Caron V. & Nelson C. S. (2009) - *Diversity of neomorphic fabrics in New Zealand Plio-Pleistocene cool-water limestones: insights into aragonite alteration pathways and controls.* J. Sediment. Res., **79**, 226-246.

Caswell B.A. & Coe A.L. (2012) - *A high-resolution shallow marine record of the Toarcian (Early Jurassic) Oceanic Anoxic Event from the East Midlands Shelf, UK.* Palaeogeogr. Palaeoclimatol. Palaeoecol., **365**, 124-135.

Cecca F., Martin-Garin B., Marchand D., Lathulière B. & Bartolini A. (2005) - *Palaeoclimatic control of biogeographic and sedimentary events in Tethyan and peri-Tethyan areas during the Oxfordian (Late Jurassic).* Palaeogeogr. Palaeoclimatol. Palaeoecol., **222**, 10-32.

Cherns L. & Wright V.P. (2009) - *Quantifying the impacts of early diagenetic aragonite dissolution on the fossil record.* Palaios, **24**, 756-771.

Clari P.A., Pierre F.D. & Martire L. (1995) - *Discontinuities in carbonate successions: identification, interpretation and classification of some Italian examples*. Sediment. Geol., **100**, 97-121.

Clari P.A. & Martire L. (1996) - *Interplay of cementation, mechanical compaction, and chemical compaction in nodular limestones of the Rosso Ammonitico Veronese (Middle-Upper Jurassic, northeastern Italy).* J. Sediment. Res., **66**, 447-458.

Coimbra R. & Olóriz F. (2012) - *Contrast comparison of differential diagenetic pathways of Lower Tithonian carbonate materials from the Betic Cordillera (S. Spain): Evidence for physico-chemical paleo-seawater properties.* Palaeogeogr. Palaeoclimatol. Palaeoecol., **321**, 65-79.

Coimbra R., Immenhauser A., Olóriz F., Rodríguez-Galiano V. & Chica-Olmo M. (2015) - *New insights into geochemical behaviour in ancient marine carbonates (Upper Jurassic Ammonitico Rosso): Novel proxies for interpreting sea-level dynamics and palaeoceanography.* Sedimentology, **62**, 266-302.

Conti M.A. & Monari S. (1992) - *Thin-shelled bivalves from the Jurassic Rosso Ammonitico and Calcari a Posidonia Formations of the Umbrian-Marchean Apennine (Central Italy)*. Paleopelagos, **2**, 193-213.

Dickson J.A.D., Wood R.A., Al Rougha H.B. & Shebl H. (2008) - *Sulphate reduction associated with hardground: lithification afterburn*. Sediment. Geol., **205**, 34-39.

Di Stefano P., Galácz A., Mallarino G., Mindszenty A. & Vörös A. (2002) - *Birth and early evolution of a Jurassic escarpment: Monte Kumeta Western Sicily*. Facies, **46**, 273-298.

Dorschel B., Gutt J., Piepenburg D., Schröder M. & Arndt J. E. (2014) - *The influence of the geomorphological and sedimentological settings on the distribution of epibenthic assemblages on a flat topped hill on the over-deepened shelf of the western Weddell Sea (Southern Ocean).* Biogeosciences, **11**, 3797-3817.

Durlet C. & Loreau J.P. (1996) - *Inherent diagenetic sequence of hardgrounds resulting from marine ablation of exposure surfaces. Example of the Burgundy platform, Bajocian (France).* C. R. ACAD. SCI. II A, **323**, 389-396.

Ebli O. (1997) - *Sedimentation und Biofazies an passiven Kontinentalrändern: Lias und Dogger des Mittelabschnittes der Nördlichen Kalkalpen und des frühen Atlantik (DSDP site 547B, offshore Marokko).* Münch. Geowiss. Abh. A, **32**, 1-255.

Erba E., Gambacorta G. & Tiepolo M. (2019) - *The Lower Bajocian Gaetani level: lithostratigraphic marker of a potential oceanic anoxic event.* Riv. Ital. Paleontol. S., **125**, 219-230.

Etter W. (1996) - *Pseudoplanktonic and benthic invertebrates in the Middle Jurassic Opalinum Clay, northern Switzerland*. Palaeogeogr. Palaeoclimatol. Palaeoecol., **126**, 325-341.

Fürsich F.T. & Oschmann W. (1993) - Shell beds as tools in basin analysis: the Jurassic of Kachchh, western India. J. Geol. Soc. London, **150**, 169-185.

Gedl P. (2008) - *Organic-walled dinoflagellate cyst stratigraphy of dark Middle Jurassic marine deposits of the Pieniny Klippen Belt, West Carpathians.* Stud. Geol. Polon., **131**, 7-227.

Grammer G.M., Crescini C.M., McNeill D.F. & Taylor L.H. (1999) - *Quantifying rates of syndepositional marine cementation in deeper platform environments-new insight into a fundamental process*. J. Sediment. Res., **69**, 202-207.

Harbury N.A. & Hall R. (1988) - *Mesozoic extensional history of the southern Tethyan continental margin in the SE Aegean*. J. Geol. Soc. London, **145**, 283-301.

Hendry J.P. (1993) - *Calcite cementation during bacterial manganese, iron and sulphate reduction in Jurassic shallow marine carbonates*. Sedimentology, **40**, 87-106.

Ivanova D.K., Schlögl J., Tomašových A., Lathuilière B. & Golej M. (2019) - *Revisiting the age of Jurassic coral bioherms in the Pieniny Klippen Belt (Western Carpathians) on the basis of benthic foraminifers*. Geol. Carpath., **70**, 113-134.

Jach R. (2007) - *Bositra limestones-a step towards radiolarites: case study from the Tatra Mountains*. Ann. Soc. Geol. Pol., **77**, 161-170.

Jach R., Djerić N., Goričan Š. & Reháková D. (2014) - *Integrated stratigraphy of the Middle–Upper Jurassic of the Krížna Nappe, Tatra Mountains*. Ann. Soc. Geol. Pol., **84**, 1-33.

James N.P., Ginsburg R.N., Marszalek D.S. & Choquette P.W. (1976) - *Facies and fabric specificity of early subsea cements in shallow Belize (British Honduras) reefs.* J. Sediment. Res., **46**, 523-544.

James N.P. & Bone Y. (1991) - *Synsedimentary cemented calcarenite layers in Oligo-Miocene cool-water shelf limestones, Eucla platform, Southern Australia*. J. Sediment. Petrol., **62**, 860–872.

Jansa L.F., Enos P., Tucholke B.E., Gradstein F.M. & Sheridan R.E. (1979) - *Mesozoic-Cenozoic Sedimentary Formations of the North American Basin; Western North Atlantic.* Deep Drilling Results in the Atlantic Ocean: continental margins and paleoenvironment, **3**, 1-57.

Jarochowska E. (2012) - *High-resolution microtaphofacies analysis of a carbonate tidal channel and tidally influenced lagoon, Pigeon Creek, San Salvador Island, Bahamas*. Palaios, **27**, 151-170.

Jefferies R.P.S. & Minton P. (1965) - *The mode of life of two Jurassic species of „Posidonia" (Bivalvia)*. Palaeontology, **8**, 156-185.

Jeleńska M., Túnyi I. & Aubrecht R. (2011) - *Low-latitude Oxfordian position of the Oravic crustal segment (Pieniny Klippen Belt, Western Carpathians): palaeogeographic implications*. Palaeogeogr. Palaeoclimatol. Palaeoecol., **302**, 338-348.

Johnson M.P., White M., Wilson A., Würzberg L., Schwabe E., Folch H., & Allcock A.L. (2013) - *A vertical wall dominated by Acesta excavata and Neopycnodonte zibrowii, part of an undersampled group of deep-sea habitats*. PloS One, **8**, e79917.

Kalin O. & Bernoulli D. (1984) - *Schizosphaerella* Deflandre and Dangeard *in Jurassic deeper-water carbonate sediments, Mazagan continental-margin (Hole-547B) and Mesozoic Tethys*. Initial Reports of the Deep Sea Drilling Project, **79**, 411-435.

Kelly S.R. & Doyle P. (1991) - *The bivalve Aulacomyella from the Early Tithonian (Late Jurassic) of Antarctica*. Antarct. Sci., **3**, 97-107.

Kidwell S.M. (1986) - *Models for fossil concentrations: paleobiologic implications.* Paleobiology, **12**, 6-24.

Kidwell S.M. (1988) - *Taphonomic comparison of passive and active continental margins: Neogene shell beds of the Atlantic coastal plain and northern Gulf of California*. Palaeogeogr. Palaeoclimatol. Palaeoecol., **63**, 201-223.

Kidwell S.M. (1989) - *Stratigraphic condensation of marine transgressive records: origin of major shell deposits in the Miocene of Maryland*. J. Geol., **97**, 1-24.

Klicpera A., Michel J. & Westphal H. (2015) - *Facies patterns of a tropical heterozoan carbonate platform under eutrophic conditions: the Banc d'Arguin, Mauritania*. Facies, **61**, 421.

Knoerich A.C. & Mutti M. (2003) - *Controls of facies and sediment composition on the diagenetic pathway of shallow-water Heterozoan carbonates: the Oligocene of the Maltese Islands*. Int. J. Earth Sci., **92**, 494-510.

Kowalewski M. (1996) - *Time-averaging, overcompleteness, and the geological record.* The J. Geol., **104**, 317-326.

Kowalewski M. & Bambach R.K. (2008) - *The limits of paleontological resolution*. In: Harries P.J. (Ed.), High-resolution approaches in stratigraphic paleontology, Springer, Dordrecht, 1-48.

Krystyn L. (1971) - *Stratigraphie, Fauna und Fazies der Klaus-Schichten (Aalenium- Oxford) in den östlichen Nordalpen*. Verh. Geol. B.-A., **3**, 486-509.

Kuhry B. (1975) - *Observations on filaments from the Subbetic of SE Spain.* Rev. Esp. Micropaleontol., **7,** 231–243.

Kuhry B., De Clercq S.W.G. & Dekker L. (1976) - *Indications of current action in Late Jurassic limestones, radiolarian limestones, Saccocoma limestones and associated rocks from the Subbetic of SE Spain*. Sediment. Geol., **15**, 235-258.

Lewandowski M., Krobicki M., Matyja B.A. & Wierzbowski A. (2005) - *Palaeogeographic evolution of the Pieniny Klippen Basin using stratigraphic and palaeomagnetic data from the Veliky Kamenets section (Carpathians, Ukraine)*. Palaeogeogr. Palaeoclimatol. Palaeoecol., **216**, 53-72.

Lopez Correa M., Freiwald A., Hall-Spencer J. & Taviani M. (2005) - *Distribution and habitats of Acesta excavata (Bivalvia: Limidae) with new data on its shell ultrastructure*. In Cold-water corals and ecosystems (eds. Freiwald A. & Roberts J.M.), Springer, Berlin, Heidelberg, p. 173-205.

Lueck R.G. & Mudge T.D. (1997) - *Topographically induced mixing around a shallow seamount*. Science, **276**, 1831-1833.

MacLeod K.G. & Orr W.N. (1993) - *The taphonomy of Maastrichtian inoceramids in the Basque region of France and Spain and the pattern of their decline and disappearance*. Paleobiology, **19**, 235-250.

Major R.P. & Wilber J.R. (1991) - *Crystal habit, geochemistry, and cathodoluminescence of magnesian calcite marine cements from the lower slope of Little Bahama Bank*. Geol. Soc. Am. Bull., **103**, 461-471.

Martire L. (1992) - *Sequence stratigraphy and condensed pelagic sediments. An example from the Rosso Ammonitico Veronese*. Palaeogeogr. Palaeoclimatol. Palaeoecol., **94**, 169-191.

Martire L. (1996) - *Stratigraphy, facies and synsedimentary tectonics in the Jurassic Rosso Ammonitico Veronese (Altopiano di Asiago, NE Italy)*. Facies, **35**, 209-236.

Martire L., Clari P., Lozar F. & Pavia G. (2006) - *The Rosso Ammonitico Veronese (Middle-Upper Jurassic of the Trento Plateau): a proposal of lithostratigraphic ordering and formalization*. Riv. Ital. Paleontol. S., **112**, 227-250.

Mazzullo S.J., Bischoff W.D. & Lobitzer H. (1990) - *Diagenesis of radiaxial fibrous calcites in a subunconformity, shallow-burial setting: Upper Triassic and Liassic, Northern Calcareous Alps, Austria*. Sedimentology, **37**, 407-425.

McRoberts C.A. (2011) - *Late Triassic Bivalvia (Chiefly Halobiidae and Monotidae) from the Pardonet Formation, Williston Lake Area, Northeastern British Columbia, Canada*. J. Paleontol., **85**, 613-664.

Michalík J., Reháková D. & Vašíček Z. (1999) - *Middle Jurassic-Lower Cretaceous pelagic sequence analysis in the Podbranč section, Pieniny Klippen Belt, Western Carpathians*. Geol. Carpath. Sp. Iss., **50**, 56-58.

Michel J., Borgomano J. & Reijmer J.J. (2018) - *Heterozoan carbonates: When, where and why? A synthesis on parameters controlling carbonate production and occurrences*. Earth-Sci. Rev., **182**, 50-67.

Mišík M. (1979) - *Sedimentological and microfacial study in the Jurassic of the Vršatec Castle Klippe (neptunic dykes, Oxfordian bioherm facies)*. Záp. Karpaty, Geol., **5**, 7-56.

Mišík M., Siblík M., Sýkora M. & Aubrecht R. (1994) - *Jurassic brachiopods and sedimentological study of the Babiná klippe near Bohunice (Czorsztyn Unit, Pieniny Klippen Belt)*. Miner. Slov., **26**, 255-266.

Molina J.M., Ruiz-Ortiz P.A. & Vera J.A. (1997) - *Calcareous tempestites in pelagic facies (Jurassic, Betic Cordilleras, southern Spain)*. Sediment. Geol., **109**, 95-109.

Molina J.M., Reolid, M. & Mattioli E. (2018) - *Thin-shelled bivalve buildup of the lower Bajocian, South Iberian paleomargin: development of opportunists after oceanic perturbations*. Facies, **64**, 19.

Monaco P. (2016) - *Ichnocoenoses and taphocoenoses of posidoniid-bearing marl-limestone rhythmites and event beds, Toarcian-Aalenian, Northern Apennines, Italy*. Geobios, **49**, 365-379.

Navarro V, Molina JM & Ruiz-Ortiz PA (2009) - *Filament lumachelle on top of Middle Jurassic oolite limestones: event deposits marking the drowning of a Tethysian carbonate platform (Subbetic, southern Spain)*. Facies, **55**, 89–102.

Negra M.H., Zagrarni M.F., Hanini A. & Strasser A. (2011) - *The filament event near the Cenomanian-Turonian boundary in Tunisia: filament origin and environmental signification*. B. Soc. Geol. Fr., **182**, 507-519.

Nelson C.S. & James N.P. (2000) - *Marine cements in mid-Tertiary cool-water shelf limestones of New Zealand and southern Australia*. Sedimentology, **47**, 609-629.

Neuweiler F. & Bernoulli D. (2005) - *Mesozoic (Lower Jurassic) red stromatactis limestones from the Southern Alps (Arzo, Switzerland): calcite mineral authigenesis and syneresis-type deformation*. Int. J. Earth Sci., **94**, 130-146.

Nieto L.M., Reolid M., Molina J.M., Ruiz-Ortiz P.A., Jiménez-Millán J. & Rey J. (2012) - *Evolution of pelagic swells from hardground analysis (Bathonian–Oxfordian, Eastern External Subbetic, southern Spain)*. Facies, **58**, 389-414.

Nohl T., Jarochowska E. & Munnecke A. (2018) - Revealing the genesis of limestone-marl alternations: a taphonomic approach. *Palaios*, **34**, 15-31.

Oschmann W. (1994) - *Adaptive pathways of benthic organisms in marine oxygen-controlled environments*. Neues Jahrb. Geol. P.-A., **191**, 393-444.

Pierre A., Durlet C., Razin P. & Chellai E.H. (2010) - *Spatial and temporal distribution of ooids along a Jurassic carbonate ramp: Amellago outcrop transect, High-Atlas, Morocco*. Geol. Soc. London, Spec.Pub., **329**, 65-88.

Plašienka D. (2019) - *Linkage of the Manín and Klape units with the Pieniny Klippen Belt and Central Western Carpathians: balancing the ambiguity*. Geol. Carpath., **70**, 35-61.

Pomar L., Morsilli M., Hallock P., Bádenas B. (2012) - *Internal waves, an under-explored source of turbulence events in the sedimentary record*. Earth-Sci. Rev., **111**, 56-81.

Pomar L., Molina J.M., Ruiz-Ortiz P.A. & Vera J.A. (2019) - *Storms in the deep: Tempestite-and beach-like deposits in pelagic sequences (Jurassic, Subbetic, South of Spain)*. Mar. Petrol. Geol., **107**, 365-381.

Préat A., Mamet B., Di Stefano P., Martire L. & Kolo K. (2011) - *Microbially-induced Fe and Mn oxides in condensed pelagic sediments (Middle-Upper Jurassic, Western Sicily)*. Sediment. Geol., **237**, 179-188.

Rais P., Louis-Schmid B., Bernasconi S.M. & Weissert H. (2007) - *Palaeoceanographic and palaeoclimatic reorganization around the Middle–Late Jurassic transition*. Palaeogeogr. Palaeoclimatol. Palaeoecol, **251**, 527-546.

Reinhold C. & Kaufmann B. (2010) *Sea-level changes as controlling factor of early diagenesis: the reefal limestones of Adnet (Late Triassic, Northern Calcareous Alps, Austria)*. Facies, **56**, 231-248.

Reijmer J.J., Bauch T. & Schäfer P. (2012) - *Carbonate facies patterns in surface sediments of upwelling and non-upwelling shelf environments (Panama, East Pacific)*. Sedimentology, **59**, 32-56.

Reolid M., Nieto L.M. & Rey J. (2010) - *Taphonomy of cephalopod assemblages from Middle Jurassic hardgrounds of pelagic swells (South-Iberian Palaeomargin, Western Tethys)*. Palaeogeogr. Palaeoclimatol. Palaeoecol., **292**, 257-271.

Reolid M., Rivas P. & Rodríguez-Tovar F. J. (2015) - *Toarcian ammonitico rosso facies from the South Iberian Paleomargin (Betic Cordillera, southern Spain): paleoenvironmental reconstruction*. Facies, **61**, 22.

Rivas P., Aguirre J. & Braga J.C. (1997) - *Entolium beds: hiatal shell concentrations in starved pelagic settings (middle Liassic, SE Spain)*. Eclogae Geol. Helv., **90**, 293-302.

Rivers J.M., James N.P. & Kyser T.K. (2008) - *Early diagenesis of carbonates on a cool-water carbonate shelf, southern Australia*. J. Sediment. Res., **78**, 784-802.

Röhl H.J., Schmid-Röhl A. & Oschmann W., Frimmel A., Schwark L. (2001) - *The Posidonia Shale (Lower Toarcian) of SW-Germany: an oxygen-depleted ecosystem controlled by sea level and palaeoclimate*. Palaeogeogr. Palaeoclimatol. Palaeoecol., **165**, 27-52.

Saller A.H. (1986) - *Radiaxial calcite in lower Miocene strata, subsurface Enewetak Atoll*. J. Sediment. Res., **56**, 743-762.

Santantonio M. (1993) - *Facies associations and evolution of pelagic carbonate platform/basin systems: examples from the Italian Jurassic*. Sedimentology, **40**, 1039-1067.

Santantonio M. (1994) - *Pelagic carbonate platforms in the geologic record: their classification, and sedimentary and paleotectonic evolution*. Am. Assoc. Petr. Geol. B., **78**, 122-141.

Santantonio M., Galluzzo F. & Gill G. (1996) - *Anatomy and palaeobathymetry of a Jurassic pelagic carbonate platform/basin system: Rossa Mts, Central Apennines (Italy). Geological implications*. Palaeopelagos, **6**, 123-169.

Santantonio M. (2002) - *Piana degli Albanesi, Monte Kumeta and the „Saccense" domain: pelagic, resedimented, and high-energy skeletal post-drowning facies from western Sicily*. In: Santantonio M. (Ed.), General Field Trip Guidebook, 6th International Symposium on the Jurassic System, Palermo, 167-219.

Schlögl J., Rakús M., Mangold C. & Elmi S. (2005) *Bajocian-Bathonian ammonite fauna of the Czorsztyn Unit, Pieniny Klippen Belt (Western Carpathians, Slovakia); its biostratigraphical and palaeobiogeographical significance*. Acta Geol. Pol., **55**, 339-359.

Schlögl J., Mangold C., Tomašových A. & Golej M. (2009) - *Early and Middle Callovian ammonites from the Pieniny Klippen Belt (Western Carpathians) in hiatal successions: unique biostratigraphic evidence from sediment-filled fissure deposits*. Neues Jahrb. Geol. P.-A., **252**, 55-79.

Segit T., Matyja B.A. & Wierzbowski A. (2015) *The Middle Jurassic succession in the central sector of the Pieniny Klippen Belt (Sprzycne Creek): implications for the timing of the Czorsztyn Ridge development*. Geol. Carpath., **66**, 285-302.

Silvestri G., Bosellini F.R. & Nebelsick J.H. (2011) - *Microtaphofacies analysis of lower Oligocene turbid-water coral assemblages*. Palaios, **26**, 805-820.

Steiger T. & Jansa L.F. (1984) - *Jurassic limestones of the seaward edge of the Mazagan carbonate platform, nortwest African continental-margin, Morocco*. Initial Reports of the Deep Sea Drilling Project, **79**, 449-491.

Steiner C., Hobson A., Favre P., Stampfli G.M. & Hernandez J. (1998) - *Mesozoic sequence of Fuerteventura (Canary Islands): Witness of Early Jurassic sea-floor spreading in the central Atlantic*. Geol. Soc. Am. Bull., **110**, 1304-1317.

Sturani C. (1967) - *Reflexions sur les facies lumachelliques du Dogger mésogéen ("lumachelle à Posidonia alpina" auctt.)*. Boll. Soc. Geol. I., **86**, 445-467.

Sturani C. (1971) - *Ammonites and stratigraphy of the Posidonia alpina beds in the Venetian Alps (Middle Jurassic, mainly Bajocian)*. Memorie degli Istituti di Geologia e Mineralogia dell' Università di Padova, **28**, 1–190.

Taylor J.D., Ormond R.F.G., Gage J.D., Angel M.V. (1997) - *Diversity and structure of tropical Indo-Pacific benthic communities: relation to regimes of nutrient input*. In Marine biodiversity: patterns and processes (eds. Ormond R.F.G., Gage J.D., Angel M.V.), Cambridge University Press, Cambridge, p. 178-200.

Tomašových A., Fürsich F.T. & Wilmsen M. (2006) - *Preservation of autochthonous shell beds by positive feedback between increased hardpart-input rates and increased sedimentation rates*. J. Geol., **114**, 287-312.

Tomašových A. & Schlögl J. (2008) - *Analyzing variations in cephalopod abundances in shell concentrations: the combined effects of production and density-dependent cementation rates*. Palaios, **23**, 648-666.

Tomašových A., Schlögl J., Biroň A., Hudáčková N. & Mikuš T. (2017) *Taphonomic clock and bathymetric dependence of cephalopod preservation in bathyal, sediment-starved environments*. Palaios, **32**, 135-152.

Tyszka J. (2001) - *Microfossil assemblages as bathymetric indicators of the Toarcian/Aalenian "Fleckenmergel" facies in the Carpathian Pieniny Klippen Belt*. Geol. Carpath., **52**, 147-158.

van Erkom Schurink, C. & Griffiths C.L. (1993) - *Factors affecting relative rates of growth in four South African mussel species*. Aquaculture, **109**, 257-273.

Van der Kooij B., Immenhauser A., Steuber T., Bahamonde Rionda J.R. & Meríno Tomé O. (2010) - *Controlling factors of volumetrically important marine carbonate cementation in deep slope settings*. Sedimentology, **57**, 1491-1525.

Van Rooij D., De Mol L., Le Guilloux E., Wisshak M., Huvenne V.A.I., Moeremans R. & Henriet J.P. (2010) - *Environmental setting of deep-water oysters in the Bay of Biscay*. Deep-Sea Res. Pt. I, **57**, 1561-1572.

Vera J.A. & Martín-Algarra A. (1994) - *Mesozoic stratigraphic breaks and pelagic stromatolites in the Betic Cordillera, Southern Spain*. In Phanerozoic stromatolites II (eds. Bertrand-Sarfati J. & Monty C.), Springer, Dordrecht, p. 319-344.

Vermeij, G.J. (1990) - *Tropical Pacific pelecypods and productivity: a hypothesis*. B. Mar. Sci., **47**, 62-67.

Waller T.R. & Stanley G.D. Jr. (2005) - *Middle Triassic pteriomorphian Bivalvia (Mollusca) from the New Pass Range, west-central Nevada: systematics, biostratigraphy, paleoecology, and paleobiogeography*. Mem. Paleontol. Soc., **61**, S79, 1-64.

Wendt J. (2017) - *A unique fossil record from neptunian sills: the world's most extreme example of stratigraphic condensation (Jurassic, western Sicily)*. Acta Geol. Pol., **67**, 163-200.

Wierzbowski A., Jaworska M. & Krobicki M. (1999) - *Jurassic (Upper Bajocian-lowest Oxfordian) ammonitico rosso facies in the Pieniny Klippen Belt, Carpathians, Poland: its fauna, age, microfacies and sedimentary environment*. Stud. Geol. Polon., **115**, 7-74.

Wierzbowski A., Aubrecht R., Krobicki M., Matyja B.A. & Schlögl J. (2004) - *Stratigraphy and palaeogeographic position of the Jurassic Czertezik Succession, Pieniny Klippen Belt (Western Carpathians) of Poland and Eastern Slovakia*. Ann. Soc. Geol. Pol., 74, 237-256.

Zempolich W.G. (1993) - *The drowning succession in Jurassic carbonates of the Venetian Alps, Italy: a record of supercontinent breakup, gradual eustatic rise, and eutrophization of shallow-water environments*. Am. Assoc. Petr. Geol. Mem., **57**, 63–105.

Manuscript received 19 March 2019; accepted 21 August 2019; published online 23 September 2019;
editorial responsibility and handling by M. Brandano